2016-07

Impact analysis of low velocity to composite box containing water

South, Taylor J.; Yun, Kyoung Jae; Kwon, Young W.

Monterey, California. Naval Postgraduate School

NPS-MAE-16-001

NAVAL POSTGRADUATE SCHOOL

MONTEREY, CALIFORNIA

IMPACT ANALYSIS OF LOW VELOCITY TO COMPOSITE BOX CONTAINTING WATER

By

Taylor J. South, Kyoung Jae Yun and Young W. Kwon

July 2016

Approved for public release; distribution is unlimited

THIS PAGE INTENTIONALLY LEFT BLANK

REPORT DOCUMENTATION PAGE

Form Approved
OMB No. 0704-0188

1. REPORT DATE *(DD-MM-YYYY)*	**2. REPORT TYPE**	**3. DATES COVERED** *(From-To)*
July 2016	Technical Report	July 2015 – July 2016

4. TITLE AND SUBTITLE

Impact Analysis of Low Velocity to Composite Box Containing Water

5a. CONTRACT NUMBER

5b. GRANT NUMBER

5c. PROGRAM ELEMENT NUMBER

6. AUTHOR(S)

Taylor J. South
Kyoung Jae Yun
Young W. Kwon

5d. PROJECT NUMBER

5e. TASK NUMBER

5f. WORK UNIT NUMBER

7. PERFORMING ORGANIZATION NAME(S) AND ADDRESS(ES) AND ADDRESS(ES)
Dept. of Mechanical and Aerospace Engineering
Naval Postgraduate School, 700 Dyer Rd.
Monterey. CA 93943-5000

8. PERFORMING ORGANIZATION REPORT NUMBER
NPS-MAE-16-001

9. SPONSORING / MONITORING AGENCY NAME(S) AND ADDRESS(ES)
N/A

10. SPONSOR/MONITOR'S ACRONYM(S)

11. SPONSOR/MONITOR'S REPORT NUMBER(S)

12. DISTRIBUTION / AVAILABILITY STATEMENT
Approved for public release ; distribution is unlimited

13. SUPPLEMENTARY NOTES
The views expressed in this report are those of the author and do not reflect the official policy or position of the Department of Defense or the U.S. Government.

14. ABSTRACT

A series of experimental studies were conducted for low velocity impact on a composite box containing water in order to study the Fluid-Structure Interaction (FSI). Finally, a computational study was conducted to supplement the experimental study. The water level inside the composite box was varied incrementally from 0% (i.e. no water) to 100% (full water). The impact velocity was also changed. In the experimental study, strain gages and the load cell were used to measure the strain responses at the front, side, and back surfaces as well as the impact force. The results showed that the FSI effect was significant to the structural responses depending on the water level. The effect of the baffle was different among the front, side and back surfaces. Both experimental and numerical results agreed well.

15. SUBJECT TERMS
Numerical Simulation, ALE method, Glass fiber composite, fluid structure interaction, low velocity impact, partially filled fluid container

16. SECURITY CLASSIFICATION OF:			**17. LIMITATION OF ABSTRACT**	**18. NUMBER OF PAGES**	**19a. NAME OF RESPONSIBLE PERSON**
a. REPORT	**b. ABSTRACT**	**c. THIS PAGE**			Young W. Kwon
Unclassified	Unclassified	Unclassified	Unclassified	77	**19b. TELEPHONE NUMBER** ***(include area code)*** 831-656-3468

Standard Form 298 (Rev. 8-98)
Prescribed by ANSI Std. Z39.18

THIS PAGE INTENTIONALLY LEFT BLANK

NAVAL POSTGRADUATE SCHOOL
Monterey, California 93943-5000

Ronald A. Route
President

James Newman
Acting Provost

The report entitled "*Low velocity impact to composite box containing water*" was prepared and funded by Naval Postgraduate School.

Further distribution of all or part of this report is authorized.

This report was prepared by:

_____
South J. Taylor
U.S Navy
Mechanical & Aerospace Engineering

_____
Kyoung Jae Yun
Visiting Scientist
Mechanical & Aerospace Engineering

_____
Young W. Kwon
Distinguished Professor
Mechanical & Aerospace Engineering

Reviewed by:

_____
Garth V. Hobson, Chairman
Mechanical & Aerospace Engineering

Released by:

_____
Jeffrey D. Paduan
Dean of Research

THIS PAGE INTENTIONALLY LEFT BLANK

ABSTRACT

An experiment was designed and conducted to study the effects of fluid structure interaction in a fluid filled cubic composite structure subjected to low velocity impact. A fabrication technique was developed for creating a composite cubic structure and an experimental set-up for analyzing a low velocity impact was designed and built. The behavior of the composite structure was studied at various fluid fill levels and impact velocities. The fluid level inside the structure was varied incrementally from empty (0% fill) to full (100% fill). With impact load measurements, strain measurements on each side, and high speed video, the behavior for each test case was analyzed and compared. The results showed the effect of fluid structure interaction in the composite was significant and varied with the fluid fill level. Finally, a computational study was compared to the experimental study. The water level inside the composite box was varied incrementally from 0% (i.e. no water) to 100% (full water). The impact velocity was also changed. In the experimental study, strain gages and the load cell were used to measure the strain responses at the front, side, and back surfaces as well as the impact force. Likewsie, similar quantities were computed using the numerical study. The results showed that the FSI effect was significant to the structural responses depending on the water level. The effect of the baffle was different among the front, side and back surfaces. Both experimental and numerical results agreed well.

THIS PAGE INTENTIONALLY LEFT BLANK

TABLE OF CONTENTS

LIST OF FIGURES

LIST OF TABLES

THIS PAGE INTENTIONALLY LEFT BLANK

I. INTRODUCTION

A. BACKGROUND

Composite materials are becoming increasingly popular as they provide high stiffness and strength with low weight. They have a range of applications in the commercial and defense sectors, especially in the aerospace and marine environment. As these applications are usually in a dynamic setting, impact loading is a major area of interest. Composite structures are generally more vulnerable to impact damage than metallic structures due to their reduced hardness and ductility. These properties allow metals to absorb greater amounts of energy without failure [1]. In addition, as composite structures are generally more flexible, greater deformation can occur following an impact. This can be a very important consideration when the composite structure in close proximity to other structures or components. For instance, due to the limited space in an aircraft the fuel cell is often situated close to vital components. In the event of impact to the fuel cell, large deformations in the structure could cause unwanted contact with the adjacent components. Even if failure does not occur in the composite structure, the dynamic response to the impact could cause damage to adjacent components. Figure 1 shows a representative fuel cell in a military helicopter.

Composite structures containing a fluid, like a fuel cell, are subject to a dynamic interaction between the fluid and the structure, called fluid–structure interaction (FSI). This effect should be considered in composites as it differs considerably from metallic structures. The difference occurs because with a metal the density of the structure is much greater than that of the fluid, namely water. In a polymer composite , the densities of the structure and fluid are comparable, resulting in a very different structural response [2].

Figure 1. Fuel cell on MH-60 Blackhawk helicopter[3]

B. OBJECTIVE

The objective of this research is to understand the FSI effect on a composite structure filled with a fluid (water) and subjected to a low velocity impact. Understanding the dynamic response of the fluid filled structure can provide important information for future composite designs. It is important to understand the conditions that cause the greatest stress, strain, and deformation in the structure as well potential mitigating factors. Ultimately, the goal of the research is to provide insight into trends that can improve defense and commercial composite structures.

C. EXPERIMENTAL OVERVIEW

An E-glass composite cubic structure was fabricated for testing and a pendulum was built to provide a repeatable low velocity impact. The effects of FSI were analyzed by incrementally varying the fluid fill level and measuring the impact force and strain

response on each side of the structure. Two baffles were designed and fabricated and their effects on the structural response were evaluated.

The composite structure was fabricated by hand wrapping E-glass fabric around a cubic form that could be disassembled after curing. A predetermined number of wraps of the composite were used to achieve a wall thickness of approximately 2 mm. Biaxial strain gages were installed at the center of the side and back faces, and offset on the front (impact) face.

Impact tests were performed for various fluid fill levels including empty (0%), 25%, 50%, 75%, 90%, 95%, and full (100%). The impact was varied between a 25 degree drop angle and a 45 degree drop angle. The tests were repeated a minimum of six times to ensure consistency among the data. Adequate time was given between each impact to ensure that there was no residual fluid motion from the previous test.

D. PRIOR RESEARCH

The majority of previous research completed on the topic composite structural impact has not considered FSI. A numerical and experimental study conducted by Kim et al. [4] is an example of a case in which a composite structure was studied without the influence of FSI. In this study impact force, deflection, and strain were measured in a carbon fiber reinforced polymer (CFRP) composite cylinder subjected to low velocity impact without the presence of a fluid. In some selected composite studies [5-7], FSI on a flat plate subjected low velocity was analyzed. In two of these studies, the composite was a sandwich construction and in the third, the composite was E-glass and resin only. The research found that FSI had a significant effect on the dynamic response of a composite structure.

Research that has included structures containing a fluid have differed from the current study as the previous work has examined impacts via numerical analysis, slosh dynamics, impacts on metal structures, and high velocity impacts. In a study conducted by Firouz-Abadi et al. [8], only a numerical analysis was used to measure the modal frequencies and wall pressures in a flexible laminated composite at various liquid levels. Additional numerical studies that have been conducted were compiled and compared by

Rebouillat et al. [9]. While many of them included experimental validation, the common theme among the research of partially filled liquid containers was sloshing effects. Sloshing seems to be the dominant area research related to composites structures filled with liquid. The experimental studies that have been conducted use a horizontal shaking excitation instead of a structural impact [10]. The effects of baffles have also been studied in these cases to determine their effect on sloshing but not due to an impact [11].

When impacts on partially fluid filled containers have been studied it has either related to metal structures or high velocity impacts to composites. In a study conducted by Ince et al. [12], low velocity impacts were analyzed but the method and materials differed from the content of the research at hand. The box structures were constructed of steel and aluminum, and the impact force was applied by dropping the box structure from an elevated position vice striking it with a mass. Finally, research conducted by Artero-Guerrero et al. [13-15] was the most comparable in many ways. In his study fluid filled CFRP rectangular structures were measured for strain and pressure during a high velocity impact at various liquid levels. Because the impact was at high velocity, the focus of the research was on hydraulic ram effects on the fluid and structure. There has been little research to date on fluid filled composite structures subjected to low velocity impact.

II. EXPERIMENTAL AND NUMERIACL RESULTS

A. COMPOSITE MATERIAL AND PROPERTIES

Composite structures can be constructed of many different materials, but many common marine and aerospace structures are made of E-glass woven fabrics and an epoxy. Within these materials lie various types that can be selected based on the specific application. Each of the various material types have different properties associated with them. The discussion below provides specific details for the properties of the materials used to fabricate the composite structure for this experiment.

1. E-glass

The E-glass woven fabric used to fabricate the composite structure was a 6 ounce bi-directional woven fabric as shown in Figure 2. This woven fabric is common with in the fiberglass industry and can be purchased in a rolled form from various vendors.

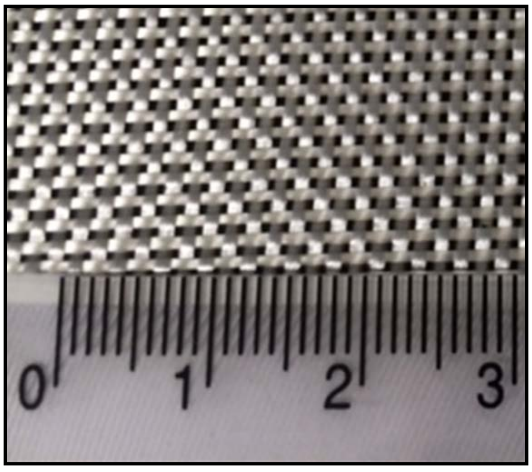

Figure 2. E-glass bi-directional oven fabric

2. E-Glass / Epoxy Composite

The e-glass and epoxy combination similar to the one used in this experiment was studied extensively by Miller [17]. In his research Pro-Set ® M237 hardener was used

vice the M2046 hardener used in this experiment. The difference between the two hardeners is the cure time. Figures 3 and 4 show the results of Miller's study. The room temperature properties are the assumed material properties for the composite structure used in this experiment.

Ultimate Strength of Composite (Pa)			
Room Temperatures		Cold Temperatures	
1–1	2.65E+08	1–2	2.47E+08
1–3	2.65E+08	1–4	2.36E+08
2–3	2.42E+08	1–5	2.76E+08
2–4	2.37E+08	2–2	2.20E+08
2–5	2.23E+08		
Average	2.46E+08	Average	2.45E+08
Standard Deviation	1.63E+07	Standard Deviation	2.05E+07
Difference (Pa)	-0.01E+08	Difference (%)	-0.4%

Figure 3. Composite ultimate tensile strength

Young's Modulus of Composite (Pa)			
Room Temperatures		Cold Temperatures	
1–1	1.02E+10	1–2	9.73E+09
1–3	1.06E+10	1–4	9.40E+09
2–3	1.00E+10	1–5	9.96E+09
2–4	1.00E+10	2–2	9.08E+09
2–5	9.95E+09	2–1*	9.06E+09
Average	1.02E+10	Average	9.44E+09
Standard Deviation	2.37E+08	Standard Deviation	3.12E+08
Difference (Pa)	7.60E+08	Difference (%)	7.45

Figure 4. Composite Young's modulus

B. COMPOSITE STRUCTURE GEOMETRY

For this experiment, a cubic geometry was selected as the structure of interest. This structural shape could be applied to many practical applications, related to previous research, and more easily modeled using numerical modeling software. The interior dimensions of the cube were chosen to be 25 cm by 25 cm by 25 cm. The walls of the cube were to be made of composite with an open top and bottom. A base plate would

support one side of the structure and the other side covered with a top plate. The desired thickness of the composite structure was approximately 2 mm. For referencing the composite structure throughout the experiment, the axes and sides were provided labels as shown in Figure 5.

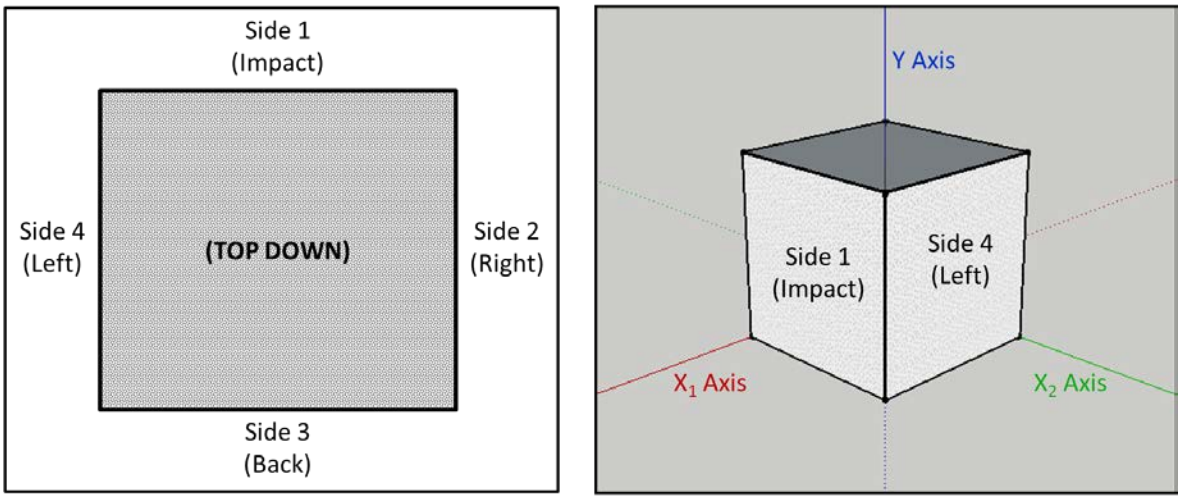

Figure 5. Side label and axis reference (a) top down view and (b) isometric view

C. COMPOSITE STRUCTURE FABRICATION

. In preparation for fabricating the cubic composite structure, past composite research projects by Violette [5], Conner [6], and McCrillis [7] were reviewed. Additionally, engineering journal articles [15, 18] were studied, and online composite structure resources were consulted [19]. It was determined that a common composite fabrication method for three-dimensional structures involved building the e-glass and resin around a form. With the e-glass and resin built around the form the entire structure would cure while under vacuum as was a common composite fabrication method in past NPS research projects.

1. Composite Form

a. Composite Layup

The form was positioned as to allow it to be rotated throughout the layup process, making the top surface the working surface. A layer of epoxy was laid to cover the wax paper and provide a surface to which the E-glass fabric could adhere. This process was repeated on each side of the form as the first layer of the E-glass was laid. Special attention was given to ensure that the first layer of E-glass and epoxy was tightly fitted around the form and especially at the corners. Figure 6 shows the first layer of E-glass fabric laid on the form.

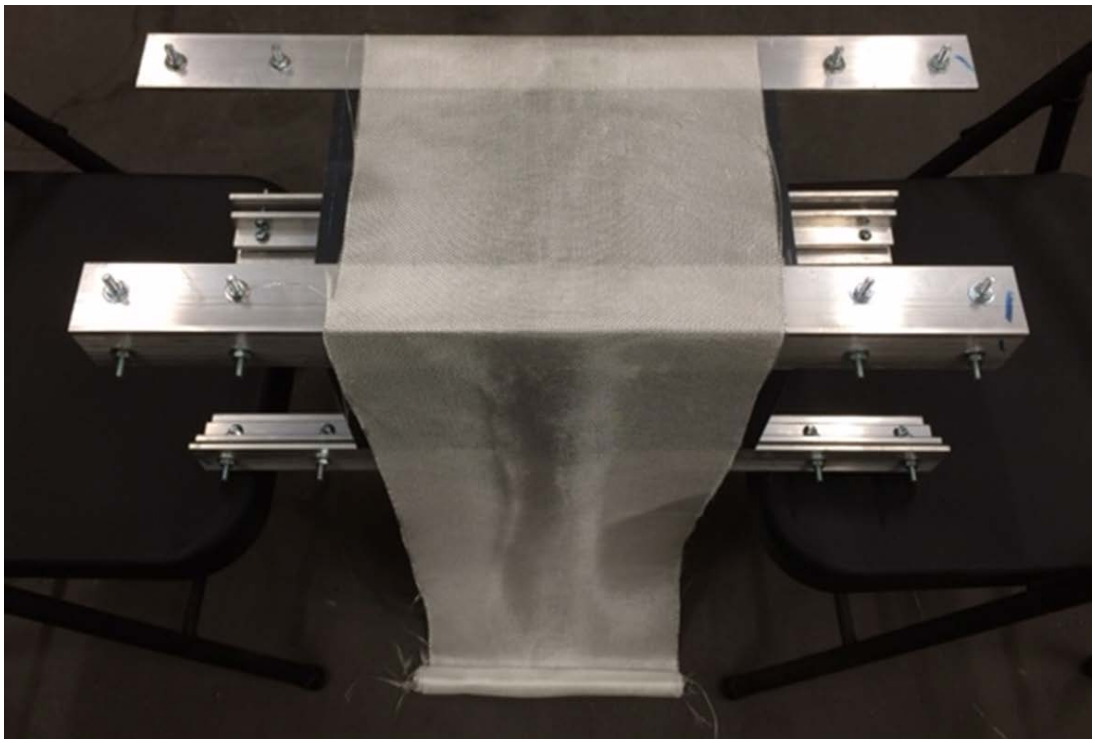

Figure 6. First layer of E-glass laid on form during fabrication

The wrapping of the E-glass layers was continued, rotating the form as each side was covered with a new layer of E-glass and thoroughly wetted with epoxy. The epoxy was poured onto the top surface (working side) and spread across the entire surface using a plastic applicator (squeegee). After the entire surface was fully wetted, any excess epoxy was moved to the next working side as the form was rotated. When the second

and third E-glass fabric sheets were added, the sheets were carefully placed so that they butt against the end of the previous sheet.

When the final layer of the E-glass fabric was laid on the form and wetted with epoxy, the composite was covered with a layer of perforated plastic. An absorbent cloth was then placed over the perforated plastic in order to removed excess epoxy when the composite was placed under vacuum. Figure 7 shows the layers of materials used in the composite layup.

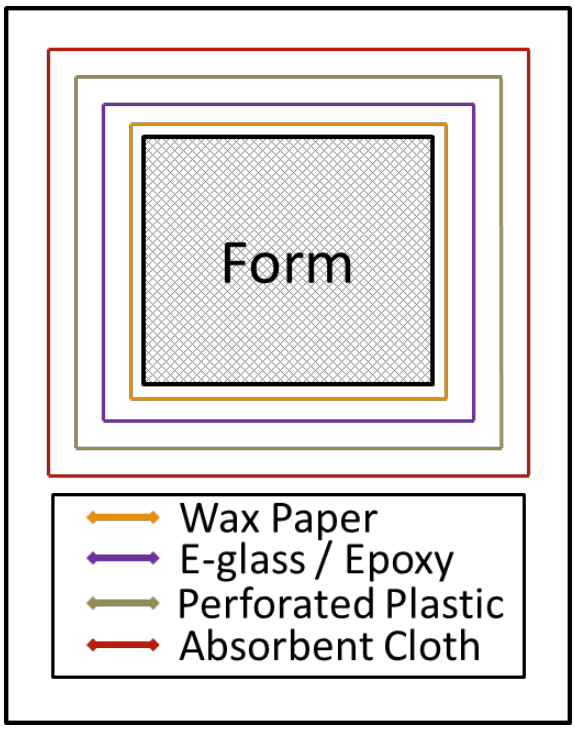

Figure 7. Material layers for composite fabrication

b. Vacuum Set-up

After completing the fabrication of the composite structure, and with all layers of materials added (Figure 7 above), the form was prepared to be placed under vacuum. To prevent puncture of the vacuum bag, the sharp corners of the aluminum angle and bolt ends were covered with double-sided gasket tape. The form was then placed inside a large heavy weight trash bag, with an additional inflated bag placed in the center of the form. The inflated bag prevented the vacuum bag from collapsing into the center of the

form and tearing. The vacuum hose was inserted and made air tight with double-sided gasket tape. Finally, the composite structure was placed under 68.95 kPa of vacuum and held for 1.5 hours. The composite structure under vacuum is shown in Figure 8.

Figure 8. Form and composite under vacuum after layup

c. Composite Curing

The composite structure was allowed to cure for 24 hours after fabrication. When completely cured, the vacuum bag, absorbent cloth, and perforated plastic were removed

and discarded. The bolts were then removed from the form so that the 2.54 cm interior aluminum angle could be removed, followed by the acrylic side plates, and finally the 5.08 cm exterior aluminum angle. The wax paper that had been the boundary between the form and composite structure was then peeled from the inside of the structure.

2. Post Fabrication Preparation

The composite structure required additional work after fabrication in order to make it ready for experimental testing. The top and bottom edges of the structure were cut to provide the proper testing dimensions, and uneven areas were sanded or filled to provide a smooth and consistent surface. Then, the impact point was reinforced to support repeated impact tests, strain gages were installed for data collection, and the exterior surfaces were painted.

a. Sizing

The top and bottom edges of the composite structure were rough due to the edges of the E-glass fabric not perfectly aligning in each layer of the fabrication process. To remove this excess composite and size the structure to the dimensions needed for testing, the top and bottom were cut to a straight edge. The overall height of the box was to be 28 cm (as 1.5 cm were fixed in the base plate and 1.5 cm were fixed in the top plate). To cut the straight edges, 14 cm were measured from the center to the top and bottom of composite structure. The top and bottom edges were made square to the sides, and cut with a Dremel ® Rotary Tool fitted with a diamond cutting wheel. Figure 9 shows the composite structure after being cut to size.

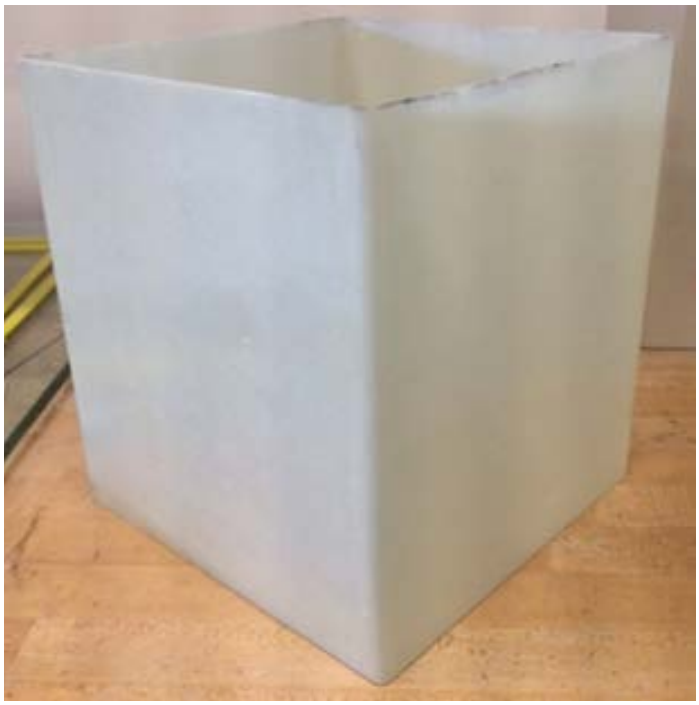

Figure 9. Composite structure cut to size for testing

b. Surface Finish

To prepare the interior and exterior surfaces of the composite structure for testing, minor finishing was needed. Several areas required epoxy filling and several areas required light sanding. The epoxy filling was required on the inside corners of the structure. Through the fabrication and curing process several voids were developed, two of which can be seen in Figure 10.

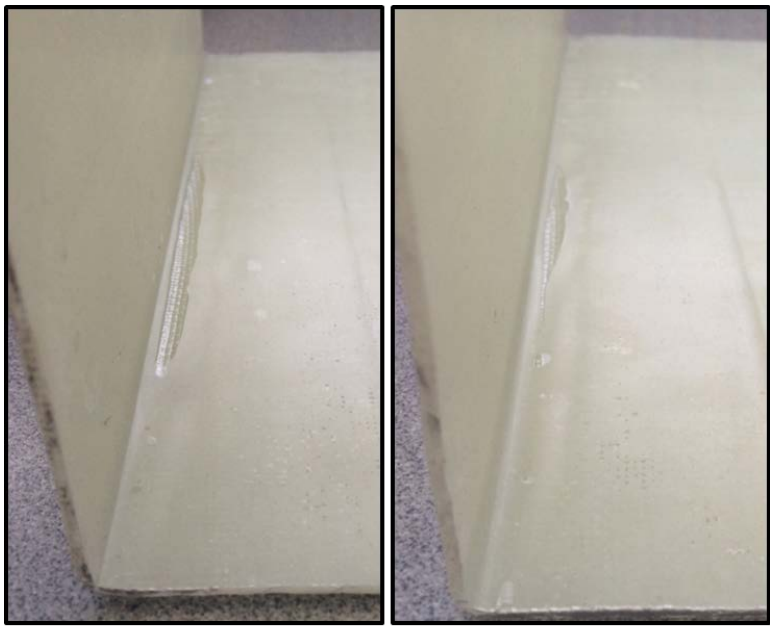

Figure 10. Examples of resin voids in the interior corners at the (a) front-right side and (b) back-left side

Because the voids were located on multiple faces, they were filled one at a time and allowed to completely cure before moving to the next face. The epoxy ratios for each void fill are listed in Table 1.

Table 1. Ratio of epoxy used to fill the voids

Void Fill	Resin	Hardener
Void Fill 1	60.0 g	15.5 g
Void Fill 2	11.6 g	3.9 g
Void Fill 3	12.0 g	3.2 g
Void Fill 4	13.9 g	3.6 g

On the exterior surface of the composite structure, the absorbent cloth did not remove several high areas of epoxy during the vacuum process. These areas were lightly sanded with 500 grit sand paper making sure to not damage the E-glass fibers.

When the surface finish was in a condition that it was ready for testing, the thickness of the composite structure was measured and recorded. A digital caliper was used to measure the thickness at 3 locations on the top and bottom of each side. Figure 11 shows the locations measured and Table 2 lists their respective thicknesses. The bottom thicknesses are larger than the top thicknesses due to the gravity forces on the epoxy during the curing process. Additionally, the thicknesses on side 4 (left) are slightly greater than the other sides. This is attributed to the amount of excess epoxy that was absorbed during the vacuum bag process and curing being slightly less than that of the other sides. The average thickness for all sides was 2.114 mm.

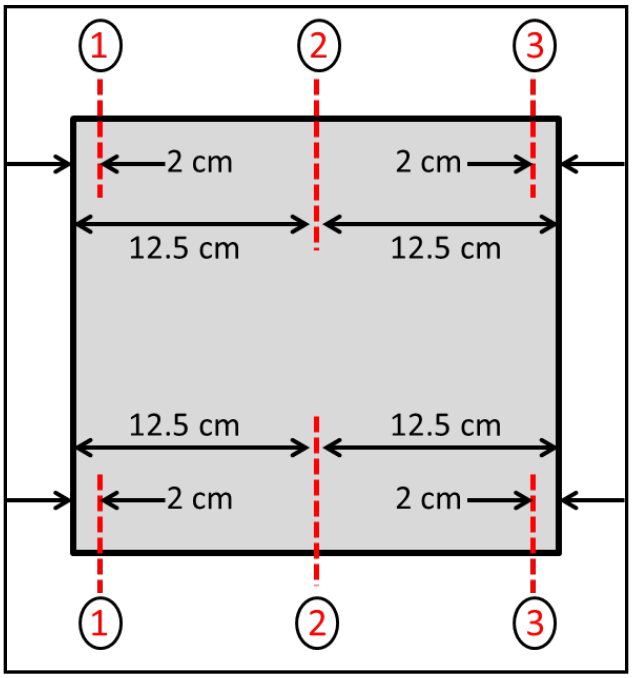

Figure 11. Thickness measurement locations

Table 2. Ratio of composite thickness mesurements

Location	Thickness	Location	Thickness
Side 1 (Impact)			
Top 1	1.76 mm	Bottom 1	2.14 mm
Top 2	1.92 mm	Bottom 2	2.32 mm
Top 3	1.99 mm	Bottom 3	2.32 mm
Side 2 (Right)			
Top 1	1.90 mm	Bottom 1	2.15 mm
Top 2	1.96 mm	Bottom 2	2.37 mm
Top 3	1.56 mm	Bottom 3	1.78 mm
Side 3 (Back)			
Top 1	1.94 mm	Bottom 1	2.16 mm
Top 2	2.06 mm	Bottom 2	2.54 mm
Top 3	1.89 mm	Bottom 3	2.29 mm
Side 4 (Left)			
Top 1	2.22 mm	Bottom 1	2.34 mm
Top 2	2.37 mm	Bottom 2	2.36 mm
Top 3	2.12 mm	Bottom 3	2.27 mm

c. Impact Point Reinforcement

Because the front face of the composite structure would experience repeated impacts during testing, the impact point was reinforced in order to prevent damage to the composite. A 3.81 cm x 3.81 cm x 0.3175 cm piece of 6061 aluminum plate was adhered to the center of the front face. The aluminum square was adhered with the same epoxy used throughout fabrication and surface finish process. Figure 12 shows the aluminum square installed at the impact point.

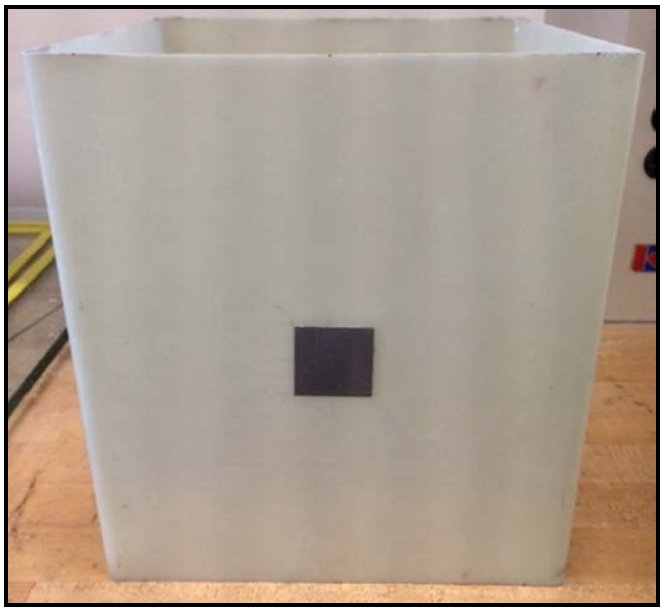

Figure 12. Aluminum impact point reinforcement

d. Strain Gage Installation

Strain gages were used to measure the strain in the x-direction and y-direction on each face of the composite structure. The strain gages were located at the center of the side faces and back face. Because the front face was impacted at the center, the strain gage on that face was offset. Figure 13 depicts where the strain gages were installed.

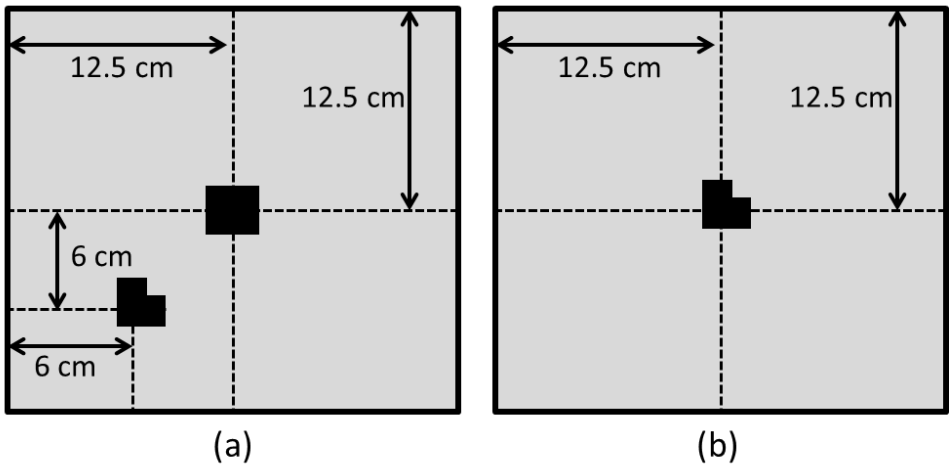

Figure 13. Strain gage locations on (a) the front side and (b) the left, right, and back

The biaxial (0° / 90°) rosette strain gages were manufactured by Micro-Measurements® (Part Number CEA-13-125WT-350). The gages had a grid resistance of 350 ohms and nominal gage factor of 2.15.

D. EXPERIMENT EQUIPMENT SET UP

The test set-up included an impact pendulum, the composite structure fixed to a base plate and top plate, strain gages and a load cell connected to a data acquisition computer, and a high speed camera.

1. Impact Pendulum

The impact pendulum consisted of four major components: a support stand, a mounting plate and rotating rod, a pendulum arm, and a hemispherical impactor with an inline load cell.

a. Pendulum Support Stand

The impact pendulum was supported by a Lateral Excitation Stand (Model 2050A) produced by The Modal Shop Incorporated [21]. The pendulum was attached to the collar on the lateral arm and could be adjusted along the length of the arm. The lateral arm was also able to be adjusted along the y-axis to ensure that the impactor was precisely aligned to the center of the composite structure. The stand was adjusted and aligned such that that the tip of the impactor was in contact with the aluminum impact plate when at rest. Because the stand was able to rotate about the y-axis, it was bolted to the test table as shown in Figure 14. The table used for the experiment was a Sealed Hole Table Top with Tuned Damping (RS 4000) supported by Stabilizer High Performance Laminar Flow Isolators (S-2000 Series) produced by Newport Corporation [22-23]. The stabilized isolators were not activated during testing.

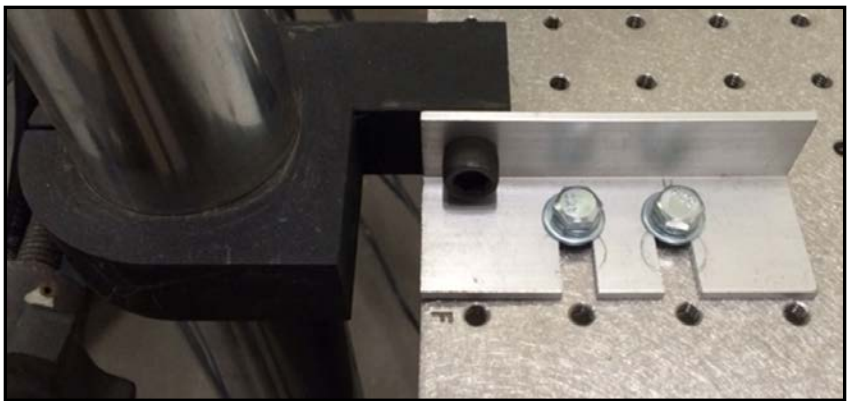

Figure 14. Impact pendulum secured to table top

b. Mounting Plate and Rotating Rod

A mounting plate was fabricated from 6061 aluminum plate that was 30.48 cm x 20.32 cm, and 0.635 cm thick. Holes were drilled through the plate as shown in Figure 15, and the plate mounted to the test stand collar using 3/8-16 U-bolts. A 6061 aluminum tube that was 30.48 cm long, with outer diameter of 2.54 cm and wall thickness of 0.635 cm, was secured in two pillow block mounted roller bearings. The roller bearings were bolted to the base plate providing the axis of rotation for the pendulum as shown in Figure 16.

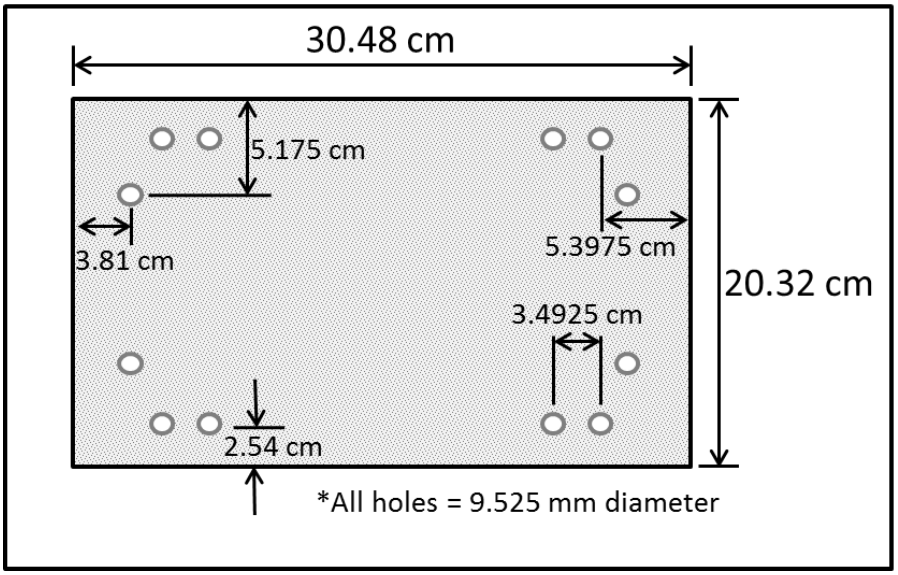

Figure 15. Mounting plate design

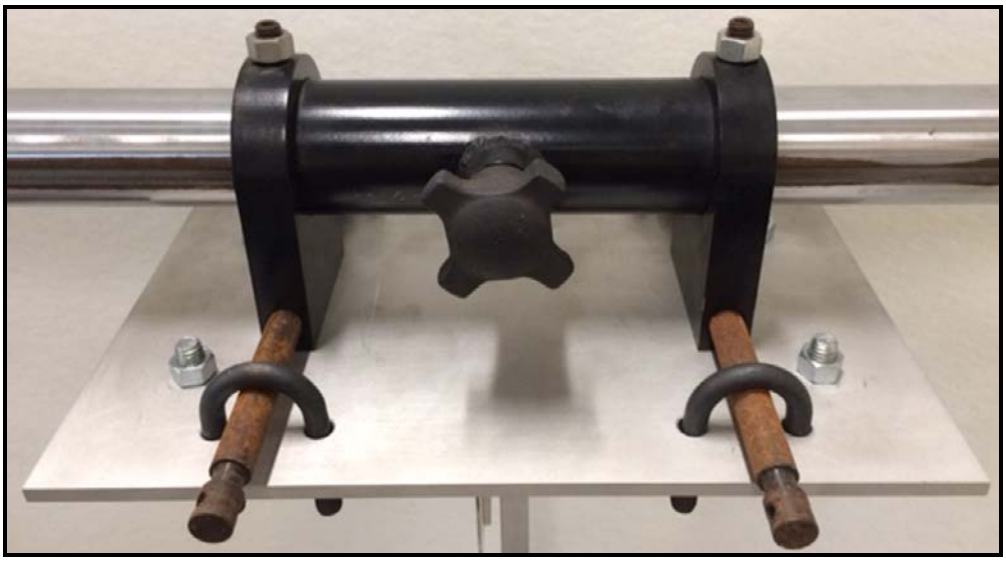

Figure 16. Mounting plate on pendulum support stand

To measure the angle of the pendulum a protractor was fixed to the bottom of the mounting plate with the 0-degree mark aligned to the center of the axis of rotation and pendulum arm, as shown in Figure 17.

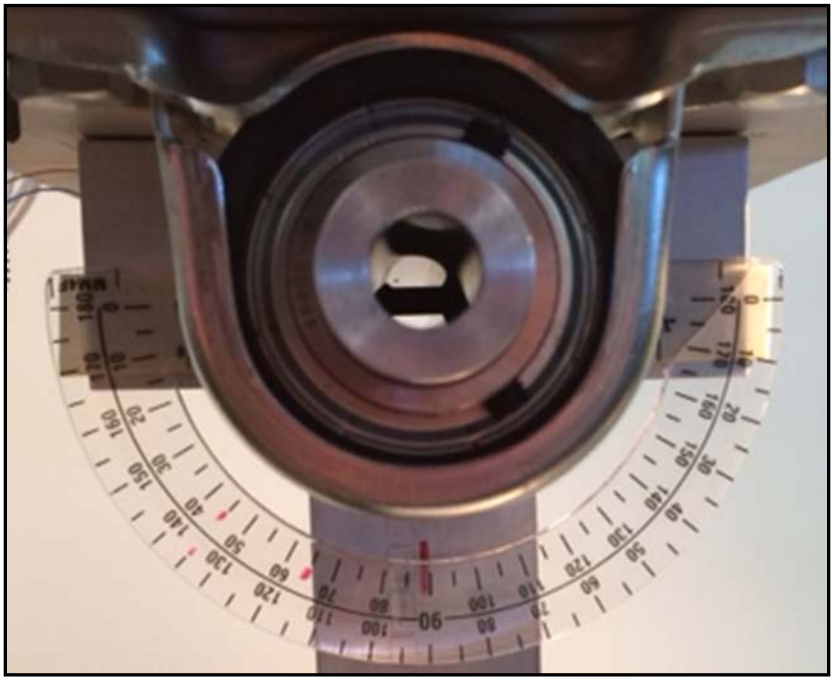

Figure 17. Protractor and pendulum arm for drop angle measurement

c. Pendulum Arm

The pendulum arm was fabricated from 6061 aluminum flat bar that measured 57.15 cm x 5.08 cm x 1.27 cm. At the top of the flat bar (arm) a 2.54 cm diameter hole was drilled to accommodate the aluminum tube (shaft). A 2.54 cm diameter hole was also drilled through the arm and shaft and fitted with a 0.9525 cm bolt and nut to bond the two pieces (Figure 18). A 2.54 cm radius was cut on the top of the arm to prevent contact with the mounting plate through the range of pendulum rotation.

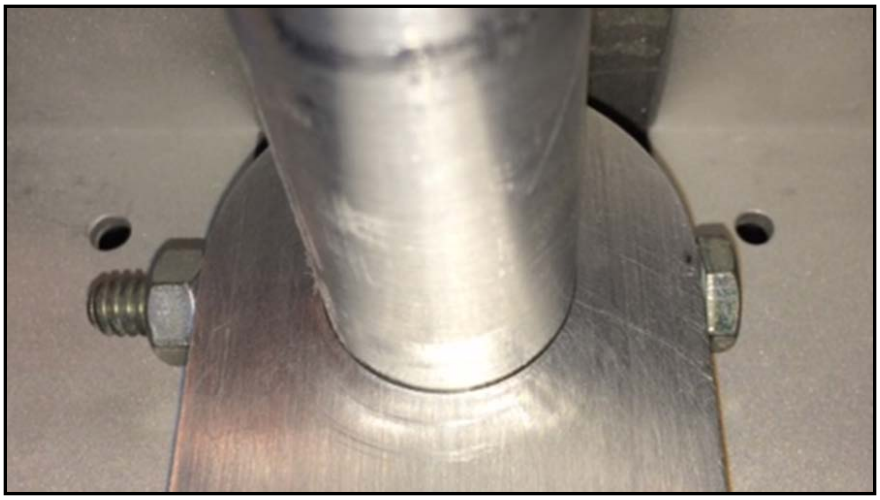

Figure 18. Attachment point for rotating rod and pendulum arm

At the bottom of the arm two holes were drilled on the back side to accommodate a brass bar for added mass. The brass bar, shown in Figure 19, measured 15.56 cm x 2.54 cm x 1.27 cm, and weighed 434.5 g. An additional hole was drilled on the front of the arm as a threaded connection point for the impactor. This hole was located 1.27 cm from the bottom of the arm; drilled to a depth of 1.27 cm and tapped for a 1/4-28 thread. The completely assembled pendulum arm is shown in Figure 20.

Figure 19. Brass weight attached to pendulum arm

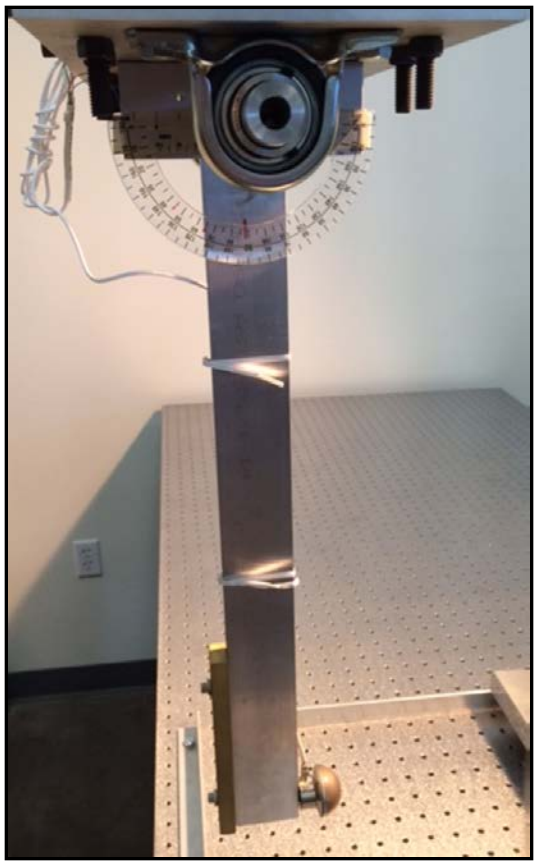

Figure 20. Complete impact pendulum set-up

d. Impactor

The impactor was fabricated using a steel hemisphere as depicted in Figure 21, and of the dimensions and properties listed in Table 3 [24].

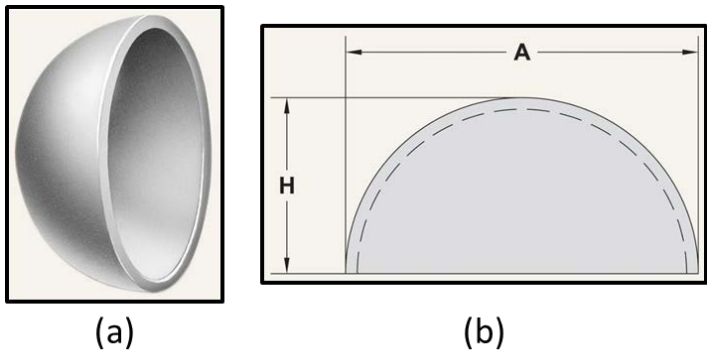

Figure 21. Steel hemisphere (a) isometric view and (b) side view

Table 3. Steel hemisphere dimensions and material property

Outside Diameter (A)	3.810 cm
Height (H)	1.905 cm
Wall Thickness	3.175 mm
Elastic Modulus	200 GPa
Density	7.87 g/cm^3
Poisson Ratio	0.29

Because the load cell had a threaded connection point, the steel hemisphere was fitted with a threaded insert to attach the hemisphere to the load cell. The insert consisted of 1/4-28 castle nut supported on a plastic sleeve of dimensions, 1.27 cm (long) x 1.429 cm (outer diameter) x 0.953 cm (inner diameter). The plastic sleeve and nut were centered in the steel hemisphere (Figure 22(a)) and secured with epoxy. When the epoxy was fully cured, the excess epoxy in the nut and sleeve were removed with a drill and tap. The completed impactor had a mass of 36.1 g and is shown in Figure 22(b).

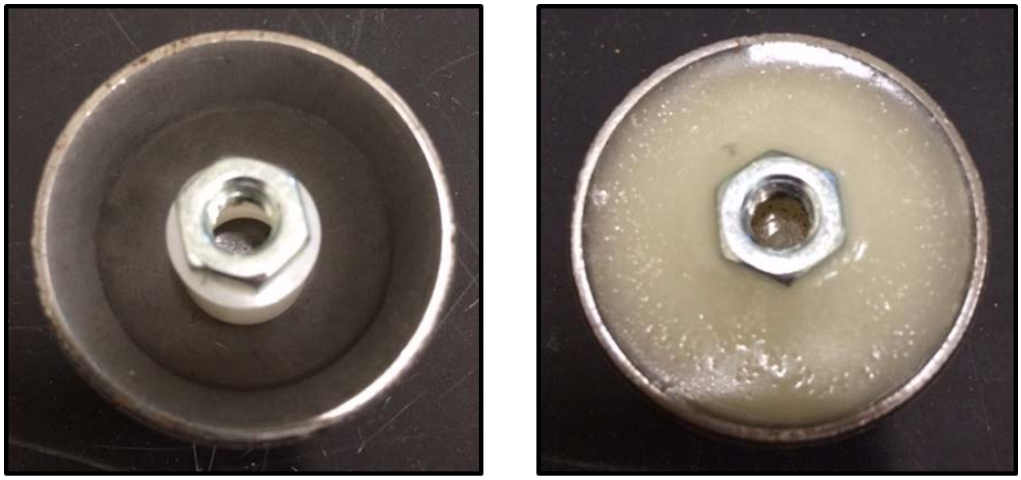

Figure 22. Impactor connection (a) set-up spacer and nut (b) filled with epoxy

2. Boundary Conditions

The composite structure was fixed between a base plate and top plate for the impact tests. The base plate was fabricated out of 45.72 cm x 45.72 cm x 2.54 cm 6061 aluminum and was considered a fixed boundary. As shown in Figure 23(a) it was also secured to the table using aluminum angle to prevent any movement. The top plate was

fabricated out of 30.48 cm x 30.48 cm x 2.54 cm acrylic glass (PMMA) and was considered a rigid boundary, as shown in Figure 23(b). A 5.08 cm hole was drilled into the corner of the top plate to allow for filling and draining the structure. The hole was tapped and could be sealed with a threaded pipe cap. Because the top plate and bottom plate were not connected to each other, the top plate was free to move based on the reaction of the composite structure. Although this was the case, minimal translation of the top plate was possible due to the rigidity of the composite.

To fit the composite structure into the base plate and top plate a groove with a 5 mm width and 1.5 cm depth was machined into both plates. The corners were radius to fit the shape of the composite structure, with the inner corner radius measuring 2.4 mm and the outer corner radius measuring 5 mm. For testing, the composite structure was inserted into the grooves and filled with silicone sealant. To ensure that the fixed boundary in the plates was very secure, 2.5 mm gasket material was pressed into the groove on the exterior of the composite structure. The structure ready for testing is shown in Figure 24.

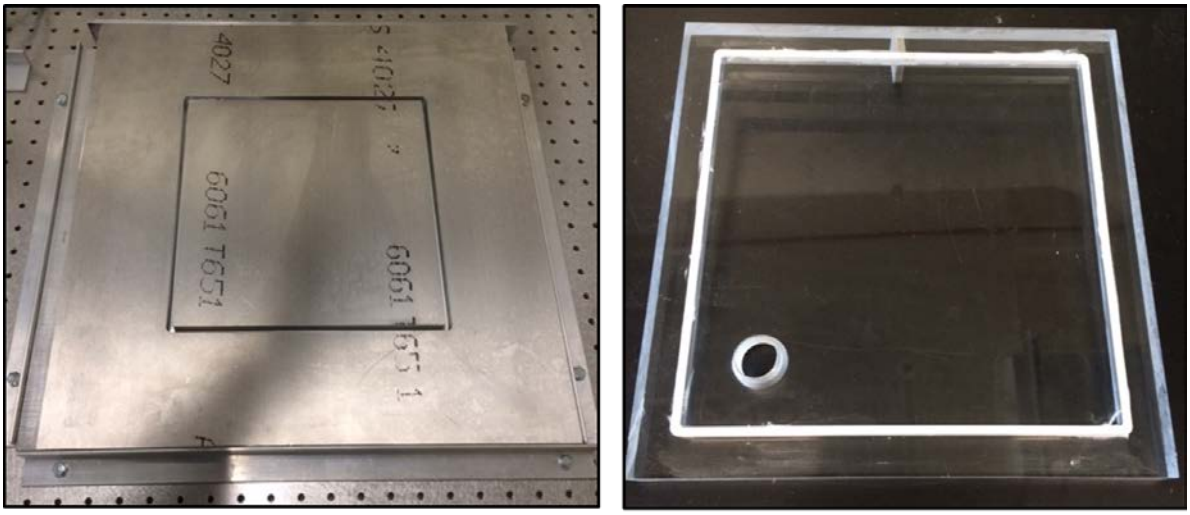

Figure 23. (a) Aluminum bottom plate and (b) PMMA top plate

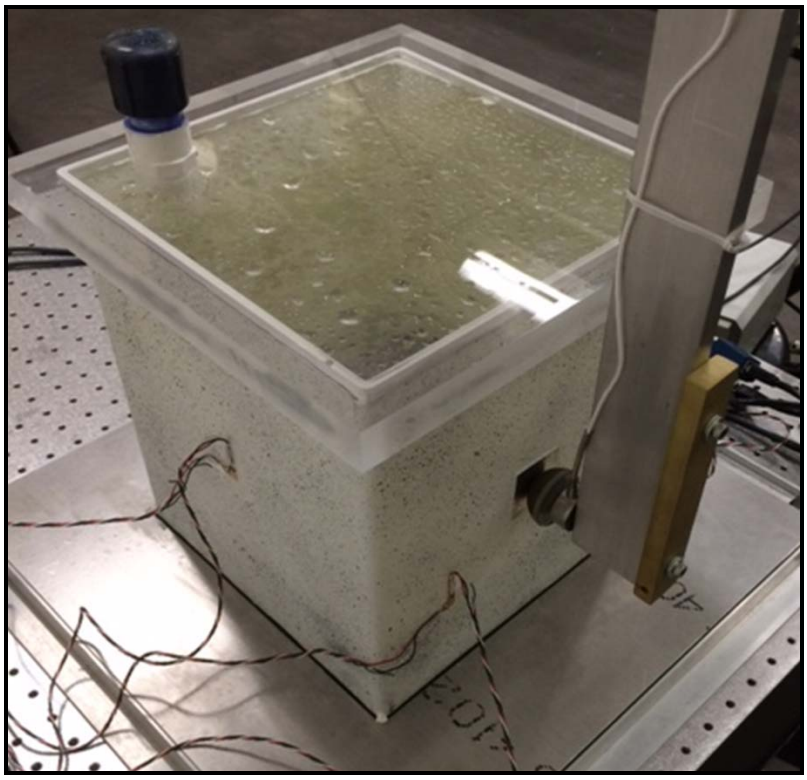

Figure 24. Complete experimental set-up

3. Strain Gages

The wired strain gages were connected to a National Instruments ® (NI) 9945 screw terminal adaptors. A screw terminal adaptor was needed for each strain gage direction (x and y axis), totaling eight adaptors. Each of the adaptors was connected to a NI 9237 bridge and strain measurement module via an RJ-50 cable. Additional details on strain gage wiring are included in the Appendix.

4. Load Cell

The load cell used to measure the impact force was a Honeywell ® Model 31 rated to 2224.1 N [500 lb-f]. It included two threaded connections as shown in Figure 25; one was connected to the end of the pendulum arm and the other connected to the impactor as can be seen in Figure 24 (above). The load cell was connected to a NI 9949 screw terminal adaptor, and like the strain gages, connected to NI 9237 bridge and strain measurement module via an RJ-50 cable.

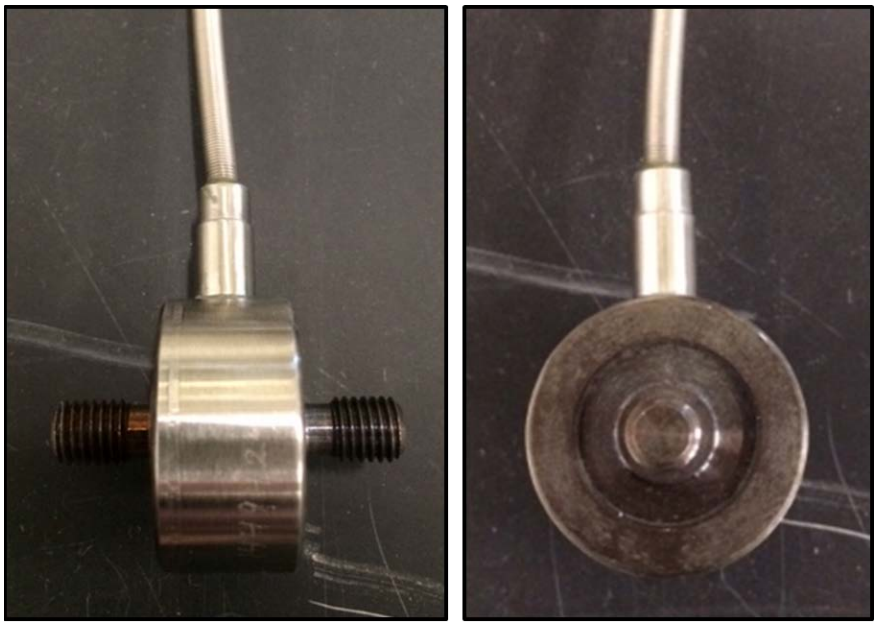

(a) (b)

Figure 25. Load cell (a) side view and (b) end view

5. Data Acquisition

The strain and impact force data were collected using the NI LabVIEW Signal Express 2012 software suite. The NI 9237 bridge and strain measurement module provided all of the inputs to the data acquisition software simultaneously. The data acquisition time interval was 20 microseconds, allowing for 67,500 samples to be read and recorded for each test run.

6. High Speed Camera

To capture the deflection of the sides of the composite structure an Olympus® i-Speed 3 high speed camera fitted with a Nikon® Nikkor 50 mm lens (Figure 26) was used. During testing, the camera was set-up to capture high speed video of the motion on the front (impact) side and back side. For these videos the camera was located at approximately a 45 degree angle from the respective face. Additionally, the motion of all sides and fluid motion was captured with the camera set-up directly above the structure as shown in Figure 27. The camera was set to capture the motion of the structure at 1,000 frames per second (fps).

Figure 26. Olympus® high speed camera, screen, and Nikon® lens

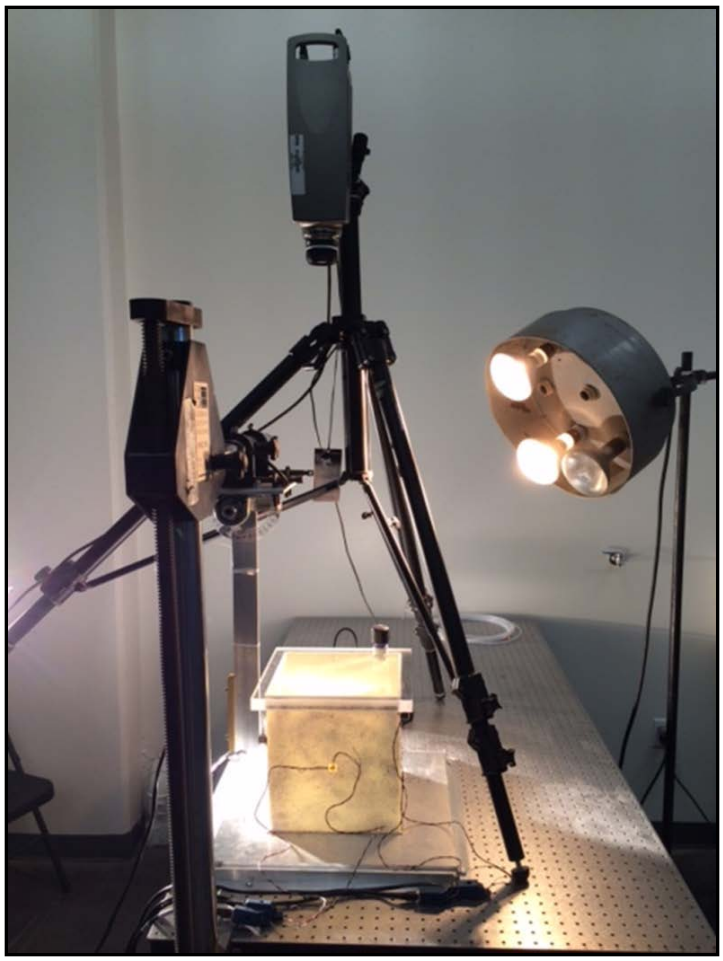

Figure 27. High speed camera set up for top-down video of side movement and fluid propagation

E. EXPERIMENTAL METHODS

To test the effects of FSI on the composite structure, tests were conducted with the structure empty (0%), full (100%), and partially filled with water. For each water level the tests were also conducted with various impact forces. The tests for each fill level and impact force combination were conducted with and without baffles installed. Every test was run repeatedly to confirm the consistency of the results.

1. Fill Level

The composite structure was filled with water incrementally between empty (0%) and full (100%). The additional fill levels that were tested were 25%, 50%, and 75%.

Following some data collection, two additional fill levels (90% and 95%) were added to the analysis in order to fully understand the strain behavior between 75% and 100%.

Because the structure was not transparent, the fill level was determined by volume. In the 100% full condition, the volume was found to be 15980 mL. This was slightly greater than the designed 25 cm cubic volume due to minor variations in the fit to the bottom plate and top plate as well as the radius of the inside corners. In the cases where a baffle was installed the volume was calculated assuming that the foam was solid since it had minimal porosity. Table 4 shows the volume associated with each fill level.

Table 4. Fill level volumes

Fill Level	No Baffle	Baffle 1	Baffle 2
25%	3995 mL	3834 mL	3673 mL
50%	7990 mL	7644 mL	7297 mL
75%	11985 mL	11453 mL	10921 mL
90%	14382 mL	13747 mL	13113 mL
95%	15181 mL	14505 mL	13829 mL
100%	15980 mL	15263 mL	14545 mL

2. Impact

Each fill case was tested with two different impact loads; one with a pendulum drop angle of 25 degrees and the other with a drop angle of 45 degrees. The 25 degree impact corresponded to a 0.959 m/s velocity and the 45 degree impact corresponded to a 1.695 m/s velocity. For the tests, the pendulum was drawn back to the desired angle as read on the protractor and released by hand. It was only allowed to impact the composite structure once; it was caught and its motion stopped as it rebounded. To ensure that the measured results were repeatable and consistent, the test was conducted six times for each drop angle at each fill level. Sufficient time was allowed between each test run for the fluid motion to return to zero.

First of all, a composite box with four sides was fabricated using E-glass woven fabric composites. The top and bottom sides were open. It had a cubic shape with the inside

dimension of 0.25 m. There was a small variation in the wall thickness. The average thickness was 2.0 mm. The bottom side of the box was closed by a 12.7 mm thick aluminum alloy plate which was attached to an optical table for vibration isolation. The top side was closed with 12.7 mm thick Plexiglas plate which had a small hole with a plug so that water could be filled inside the box. Figure 28 illustrates the box attached to an optical table. Then, a pendulum type loading unit was used to impact the composite box. The impacting pendulum had a total mass 5 kg and the length of the arm 0.5 m. The tip of the impact had a hemispherical shape. A load cell was attached to the hemispherical impactor to measure the impact force.

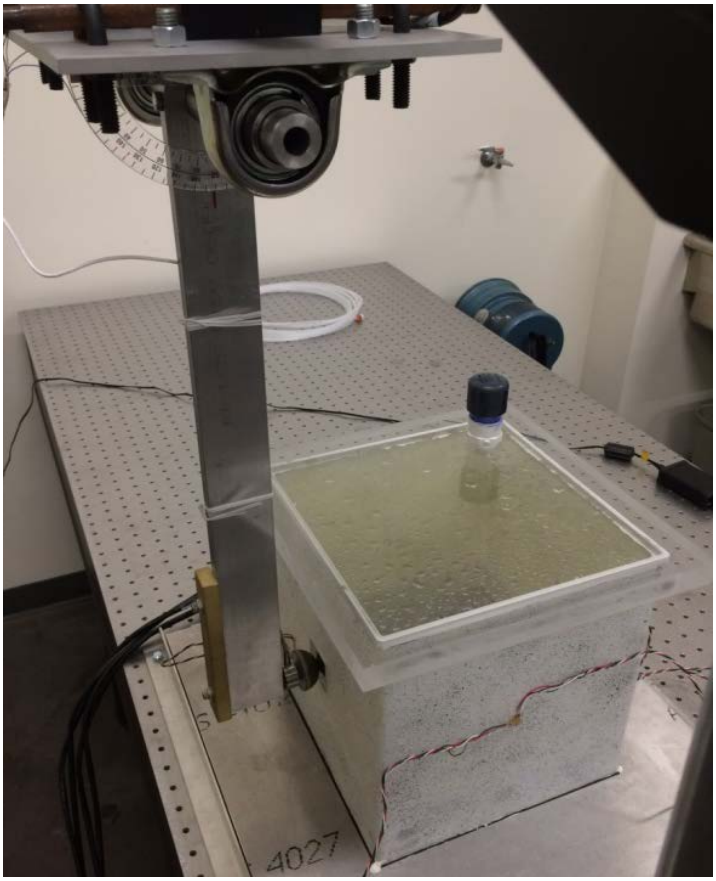

Figure 28. Experimental set-up

The impact velocity was determined by setting the pendulum at an initial angle measured from the vertical axis and letting go freely. One test was conducted with 45^{o} while the other was conducted with 25^{o}. The former resulted in the impact velocity 1.695 m/s while the latter yielded the impact velocity 0.959 m/s. The impact was applied to the center of the front face of the composite box. In order to avoid any local denting, a thin aluminum alloy plate of 25.4 mm x 25.4 mm x 2 mm was attached to the impact side of the composite box.

In order to measure strains on each side, strain gages were attached to each composite surface. Figure 29 shows the strain gage locations. All strain gages were attached at the center of each surface except for the front surface because the impact hammer struck the center location. As a result, the strain gages were fixed at the bottom left quarter point location of the front surface. Each strain gage had two measurements in the horizontal and vertical directions.

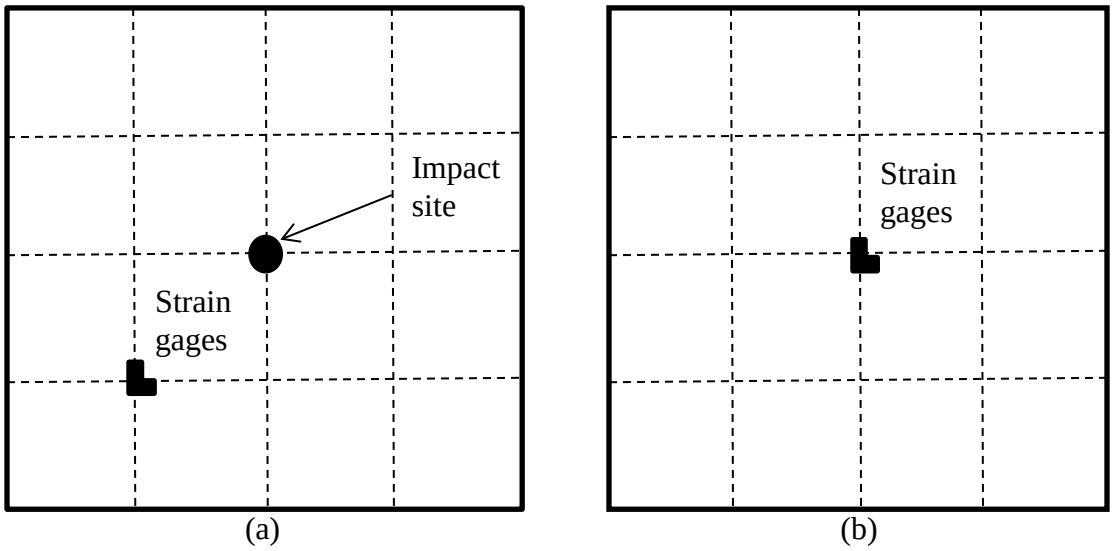

Figure 29. gage locations. (a) front surface, (b) side and back surfaces

Experimental tests were conducted while water was filled in the box incrementally. First, the empty box was tested. Then, water was filled in the box with 25%, 50%, 75% and 100%, respectively. If necessary, water was also filled in a smaller increment. Another set of tests were conducted with a baffle inserted in the box. Two different shapes of baffles were used, respectively. The two baffles are shown in Figure 3. The total opening area of each baffle was the same. The baffle was made of Divinycell vinyl form material which is much lighter than water. The first baffle was constructed of two equal size forms of 0.24 m by 0.24 m with six square shape holes in each plate. Each hole size was 0.03 m. The second baffle was made of four plates of foam. Each foam has nine opening of size 0.02 m by 0.03 m. When water was added to the box, the baffle floated and contacted the top of the box.

Every test case was repeated at least several times to determine the repeatability of the test results. Enough time was given between each test so that water became at rest without motion. The test results showed very small standard deviations confirming repeatability. The standard deviation was plotted when the test results were presented.

F. DESCRITPTION OF NUERICAL METHOD

A set of numerical studies were conducted to supplement the experimental results. Because of symmetry, one half of the box was selected for the numerical study. The symmetric plane was located at the middle between the two side surfaces. As a result, a half of the front and back surfaces were included in the computer model. The composite box was modeled using shell elements as shown in Figure 30(b). The four sides of the box had 10,359 elements. The top and bottom plates had 1,750 elements, respectively. Fine meshes were used for the impact side as well as the back side as shown in Figure 30(a).

The Impact hammer was modeled using 2,500 solid elements. The fluid was modeled using 12,300 box-shape elements. Figure 30(c) shows the full water mesh to be inserted into the box. As the water moves inside the box, some cavitation may occur. Therefore, the water was surrounded by air in the model. If the box were partially filled, the remaining empty state would be modeled using air to represent water sloshing inside the box.

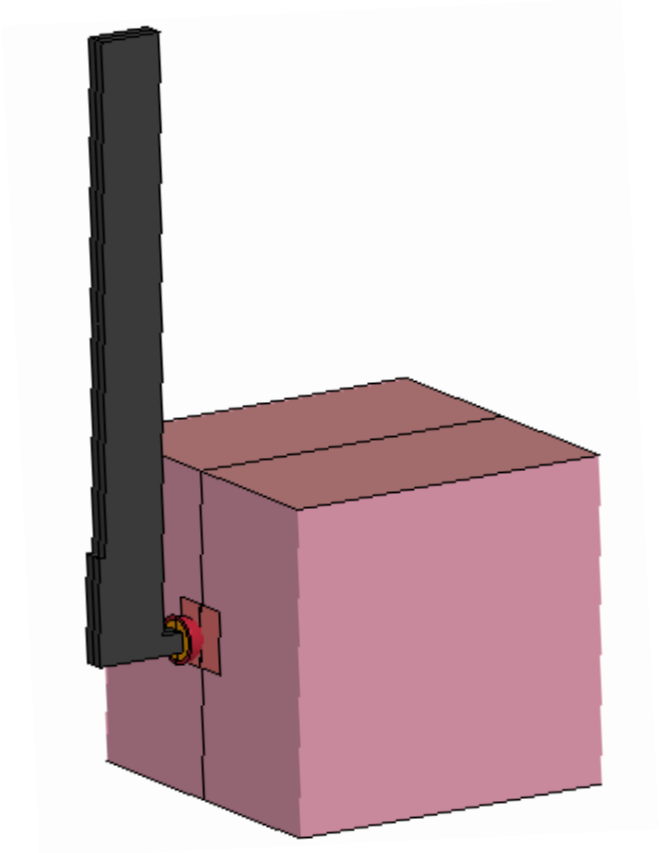

(a)

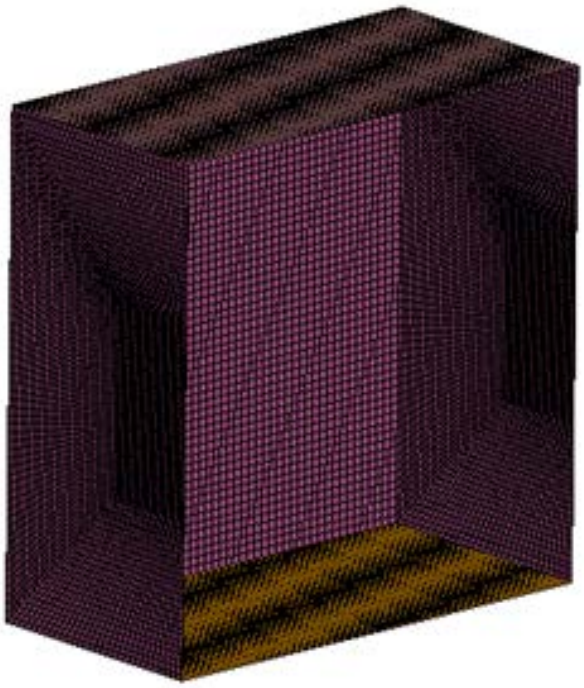

(b)

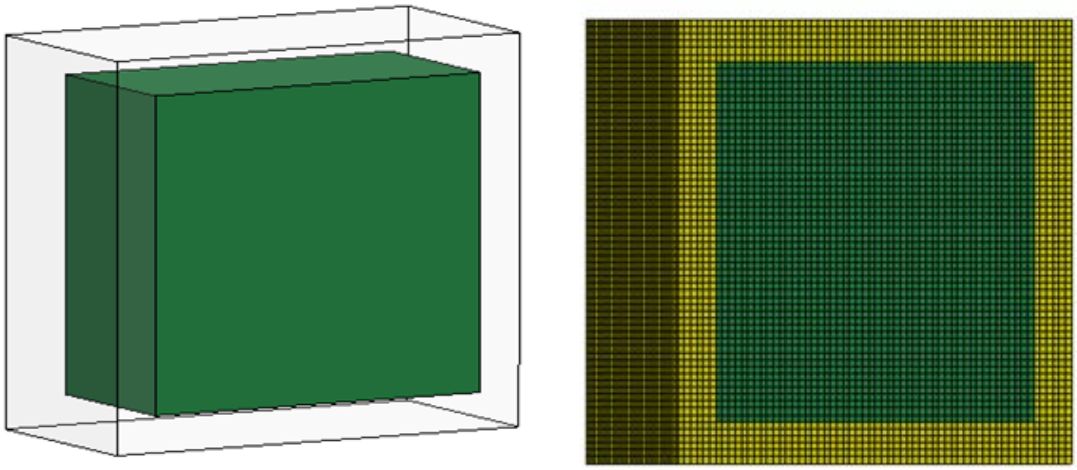

(c)

Figure 30. Finite Element Models for the (a) full model, (b) box and the (c) fluid

The woven fabric composite material had the same elastic modulus in the warp and fills directions. As a result, the composite was modeled as an isotropic material with the elastic modulus 25 GPa, Poisson's ratio 0.3, and density 1,900 kg/m^3. The bottom surface was constructed of an aluminum alloy which has elastic modulus 710 GPa, Poisson's ratio 0.33, and density 2,700 kg/ m^3. The bottom side was fully constrained from motion. Top surface was made of Plexiglas which has elastic modulus 3.0 GPa, Poisson's ratio 0.35, and density 1,180 kg/m^3.

The impact hammer was initially located just next to the impact site with the specified initial velocity. Then, the impact-contact condition was applied between the impact hammer and the composite box. We can see the initial configuration and maximum deformation of dynamic behavior for 0%, 50%, and 100% filled water box in Figure 31.

On the other hand, the Euler-Lagrangian coupling was applied to the solid and fluid interface. The numerical simulations were performed using the software LS-DYNA3D [30] which used the Arbitrary Lagrangian–Eulerian (ALE) technique to solve fluid–structure interaction problems.

(a)

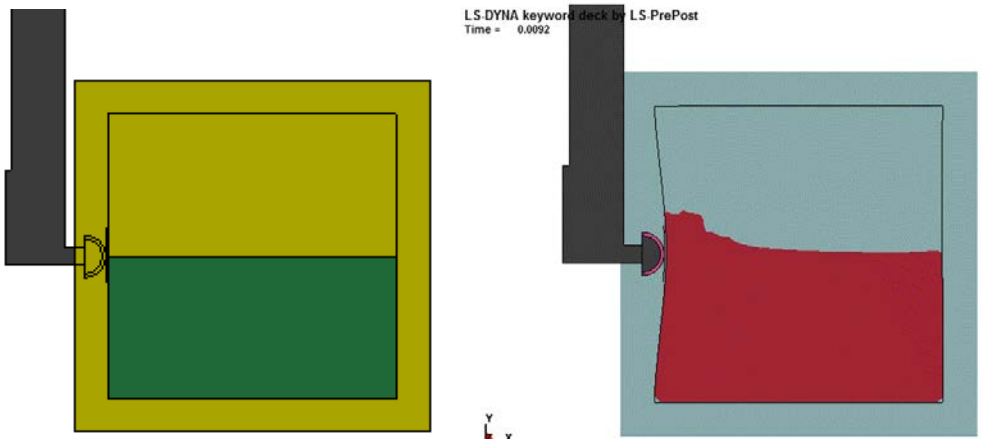

(b)

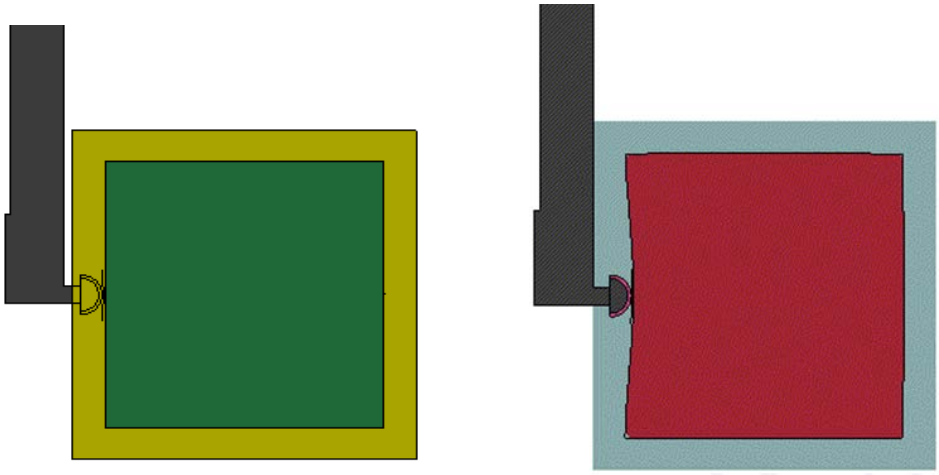

(c)

Figure 31. The initial and maximum deformation of dynamic behavior for (a) 0% water, (b) 50% filled water and (c) 100% filled water

III. RESULTS OF EXPERIMENTS AND NUMERIAL ANALYSIS

A. RESULTS OF EXPERIMENTS

All the following results are for the 45^{o} impact without baffles unless otherwise mentioned. Under the same initial impact condition like the same impact mass and impact velocity, the water level influenced the impact force applied to the front surface as shown in Figure 32.

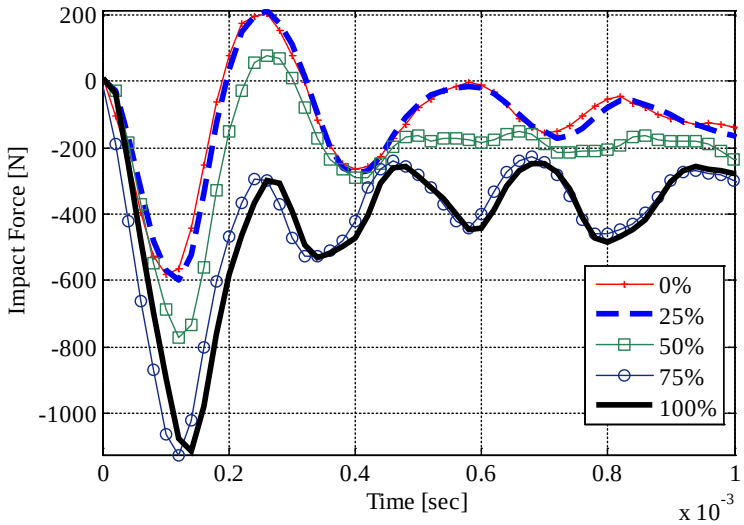

(a)

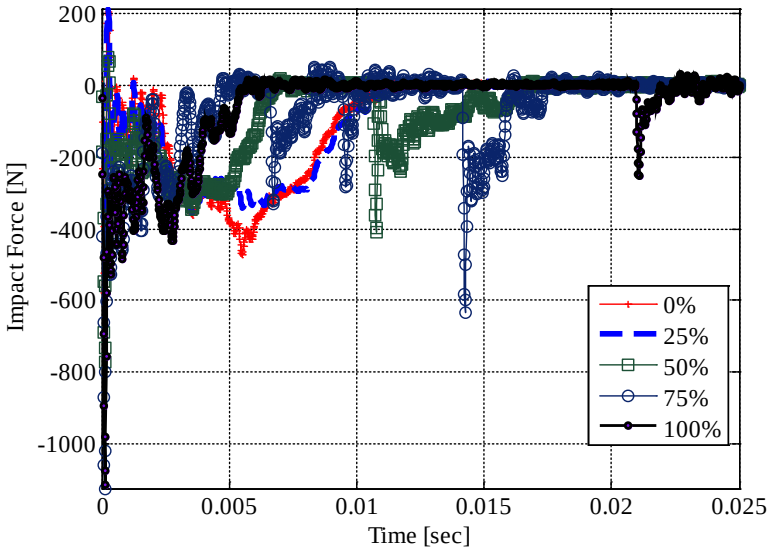

(b)

Figure 32. Plot of impact force vs. time: (a) zoom-in view (b) zoom-out view

When the water level was 25% or less called the low fill, the influence of the water was negligible on the peak impact force. On the other hand, as the water level became 75% or higher called the high fill, there was a large effect of the water on the peak impact force. However, the maximum impact force was almost constant. When the water level was at the impact location, i.e. 50% full water called the mid fill, water affected the maximum impact force whose magnitude was between the low and high fills as shown in Figure 33.

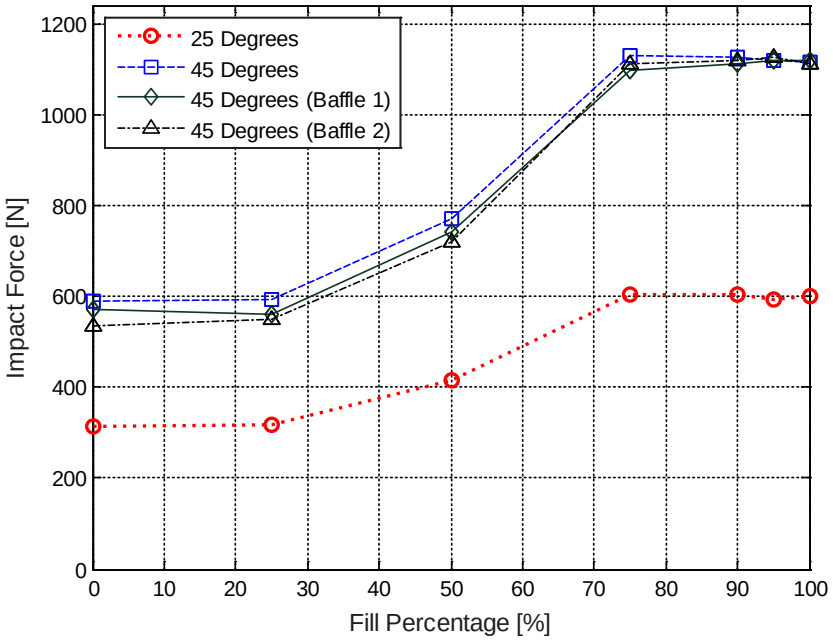

Figure 33. Plot of maximum impact force for different water fill levels

The time when the maximum impact force occurred was slightly later for the high fill compared to the low fill. However, the difference is very small. Approximately, the maximum impact force occurred at 0.12 msec. for all impact cases.

All impact forces showed oscillatory changes after their initial peak values. Then, the low fill cases had longer contact periods between the impactor and the structure than the high fill cases before their initial separation. The high fill cases showed additional contacts after separation from the initial contacts as seen in Figure 32. The motions of the composite front surface and the impactor were observed using a high speed camera with 50,000 frames per second. The video showed that the front surface of the low fill box moved like the first mode shape of a clamped plate. However, other partially filled box

clearly showed higher mode shapes superimposed on the first mode shape. Periods of higher mode shapes of the front surface are shorter and the front surface caught up the reversing impactor. The 100% full box did not show any notable higher mode shape but the front surface had a quick reverse motion compared to that of the empty box. This also resulted in additional contact after the first contact as shown in Figure 32 (b). The secondary contact occurred much later for the 100% full case as compared to others. In addition, the magnitude of the secondary impact force was the smallest for the 100% full case. The 75% full case had three contacts after the initial one. Among the three, the last contact had the greatest contact force.

The following strains are for the horizontal components unless otherwise mentioned. The strain gage location at the front surface is shown in Figure 29. As the impactor hit the center of the front surface of the box with the low fill, the front plate started to concave locally from the center. Until the concave spread further throughout the front surface, the strain gage showed tensile strain. As the concave spread out widely while the impactor was in contact with the front surface, the strain gage showed the negative strain for the contact duration. On the other hand, the strain gage for the mid and high fill cases showed the opposite behavior. It varied from compression to tension. The initial contact duration was shorter for the mid to high fills. As stated above, the mid to high fill cases had higher frequencies of motion than the low fill cases as shown in Figure 34. The maximum magnitude of the front surface strain was in compression for all the cases except for the 100% fill case which had the maximum tensile strain. The maximum strain was larger with more water fill in general. However, the 75% fill case had a slightly greater peak strain than the 100% fill case. The former occurred in compression while the latter happened in tension. The 50% full case had the maximum strain much later than other cases while the 100% full case had the earliest peak strain. The 90% and 95% full cases were plotted in Figure 35 in order not to crowd Figure 34 too much. Their behaviors were close to that of the 100% full case.

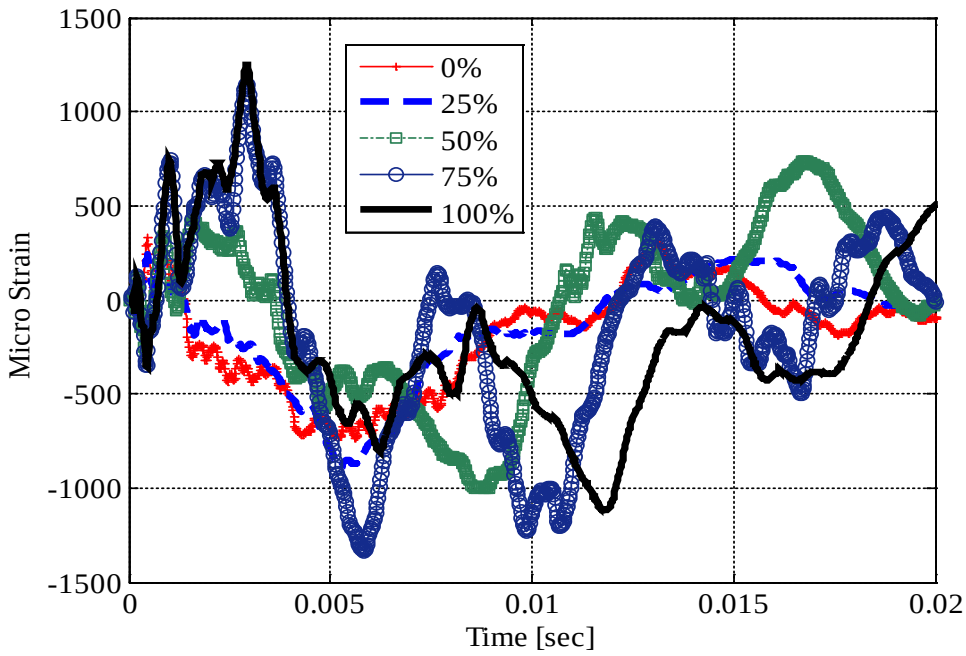

Figure 34. Plot of horizontal strain time history at the front surface

However, the 95% full case had the largest tensile strain while the 90% full case had the smallest tensile strain among the three cases as seen in Figure 34. On the other hand, the 90% full case had the greatest compressive strain while the 100% full case showed the smallest compressive strain. The peak compressive strain was greater than the peak tensile strain in terms of magnitude for the 90% case. The maximum magnitude of strain at the front surface gage was plotted as a function of the water level in Figure 36. The maximum strain increased with more water for the low and mid fill cases. However, it was different for high fill cases, and the 100% full case had the smallest strain out of the high fill cases.

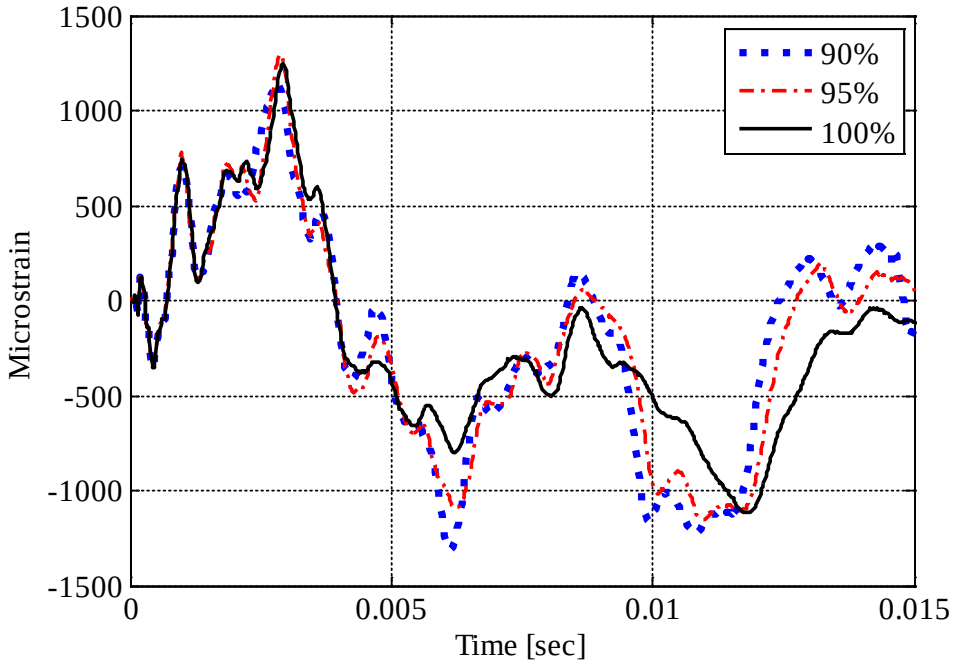

Figure 35. Plot of time history at the front surface with near full water levels

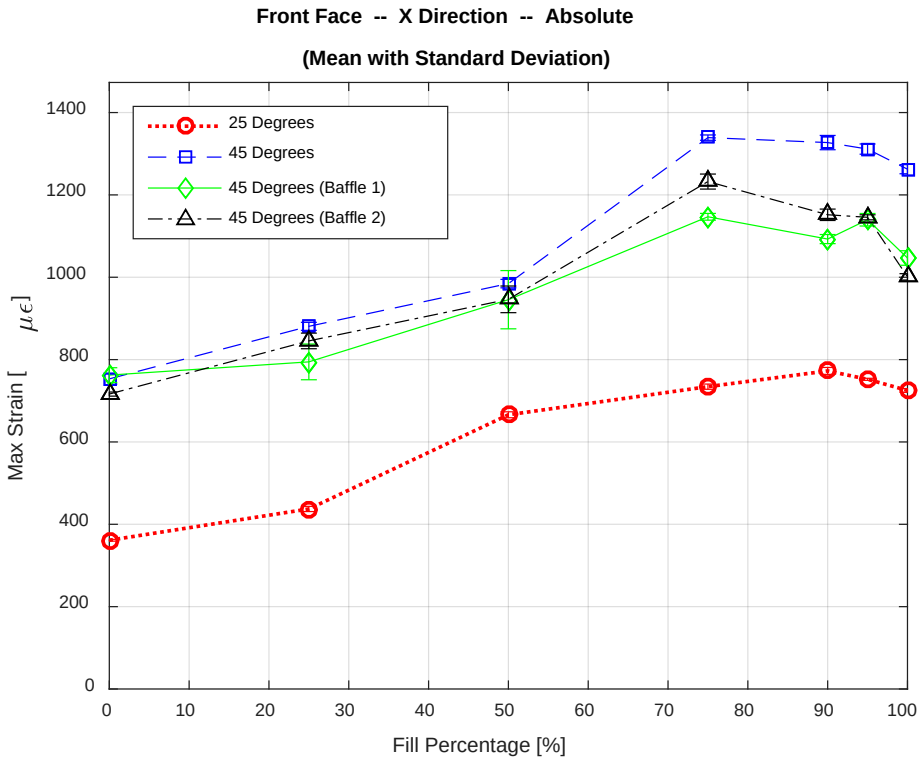

Figure 36. Plot of the maximum strain at the front surface vs. water fill level

Figure 37 plots the maximum strain in magnitude at the back surface as a function of the water level. All the maximum strains were in tension. The 50% full case had the smallest strain while 95% full case had the largest strain. The 90% and 95% full cases had the maximum strain which was more than twice of that of the 50% full case. The standard deviation was also plotted in Figure 37. The 50%, 75% and 90% full cases have larger standard deviations than other cases. Especially, the 50% full case showed the largest standard deviation.

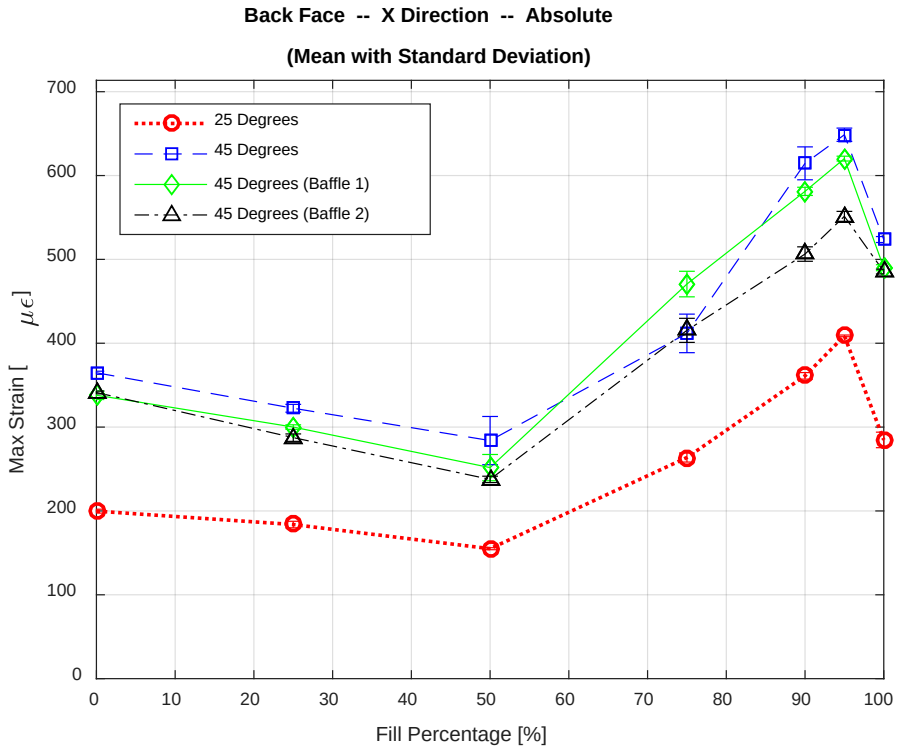

Figure 37. Plot of the maximum strain at the back surface vs. water fill level

Figure 38 shows the time when the maximum strain occurred. The maximum strain occurred earlier for the low fill cases. However, the high fill cases, except for the 100% full case, had the maximum strain at the time which occurred twice longer than that for the low fill cases. On the other hand, the 50% full case showed a huge value of standard deviation. This can be explained as follows.

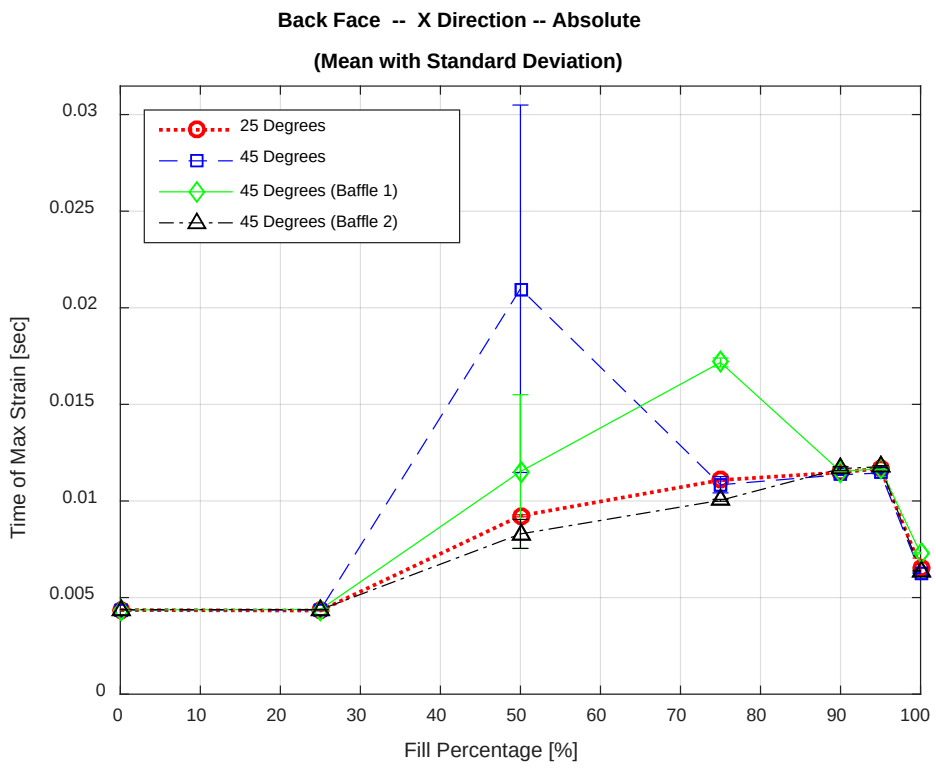

Figure 38. Plot of the time for the max strain at the back face vs. water fill

The low fill cases as well as the 100% full cases had the maximum strain at the first peak value of the strain-time plot. On the other hand, 75% to 95% full cases had the maximum strain at the second major peak. The 50% full case showed two alternative situations. One had the maximum strain at the first major peak while the other had the maximum at the second peak. More than two dozen tests were conducted for the 50% full case. Each situation occurred for the half of the tests approximately. In other words, the 50% full case showed bifurcation. In order to further test the bifurcation phenomenon, the water level was changed to 55% and 60%, respectively. Bifurcation showed up in those cases, too. To explain the phenomena, the Fast Fourier Transform (FFT) was conducted for the strain-time history plots. Figure 39 shows the FFT plot of the 50% full case. In order not to overcrowd the figure, only two representative plots were included in the figure even though two dozens of repeated tests were undertaken. The plot suggests that two major frequencies competed. One test showed that the lower frequency had the largest magnitude while another test showed that the higher frequency had the largest magnitude.

Therefore, the maximum strain was associated with the lower or higher frequency, which determined the deformation shape and the time when the maximum strain might occur.

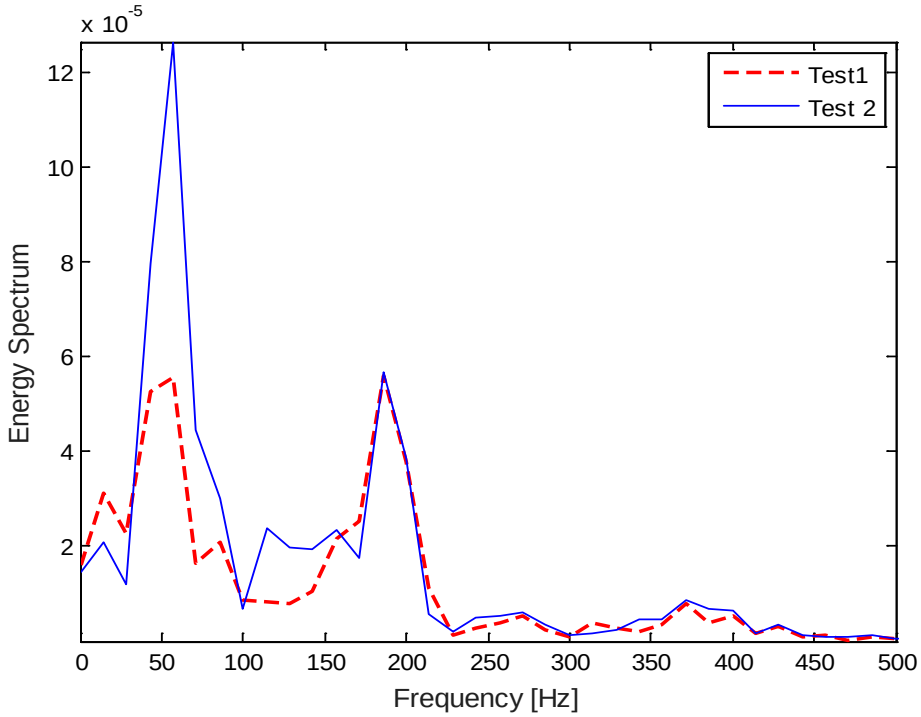

Figure 39. Plot of frequency spectrum for 15% full case

Figure 40 plots the change in the natural frequency of the composite box as a function of the water level. As the water level increased, the frequency decreased with the greater added mass effect. However, the decrease in the frequency was not linear to the increase in the water level.

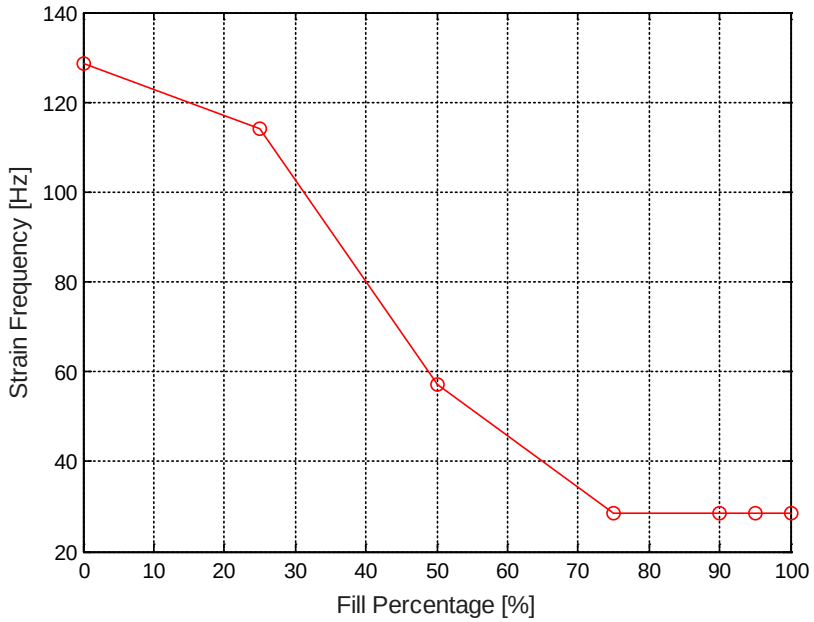

Figure 40. Plot of the lowest frequency as a function of water fill level

The next study compared the two different impact forces: one with 45^{o} and the other with 25^{o} initial setting angles. The former has the impact velocity 1.77 times greater than the latter. Figure 39 compares the impact forces. The ratio of the maximum impact forces between 45^{o} and 25^{o} initial setting angles was almost the same as the ratio of the impact velocity throughout all water levels.

B. RESULTS OF NUMERICAL ANALYSIS

The next study was the numerical result. The numerical results were compared to the experiment data so as to validate the model. Figures 41 and 43 compare the strains in the 0% filled water (empty) composite box. And Figures 44 and 46 compare the strains in the 50% filled water composite box. Finally, Figures 47 and 49 compare the strains in the 100% water-full composite box The comparison was made at the font surface, side surface, and back surface of the empty box, 50% water filled box and the 100% water-full box, respectively.

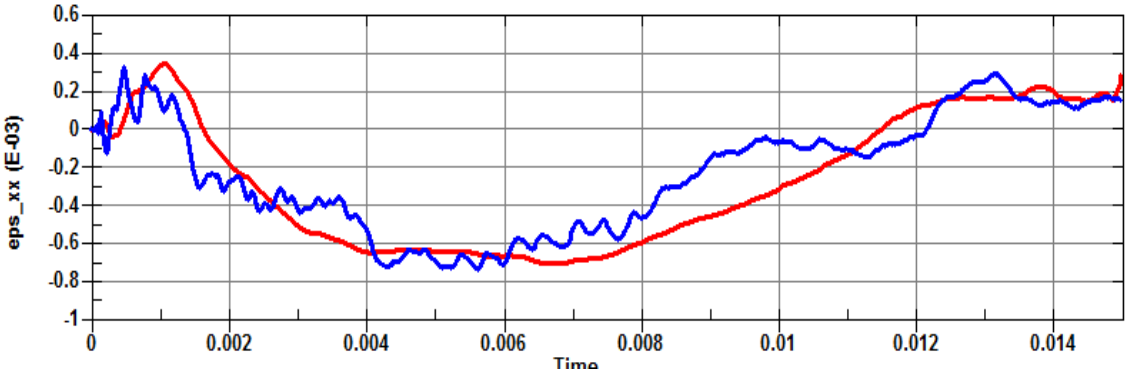

Figure 41. Comparison of strains at the front surface between the numerical and experimental results for empty box

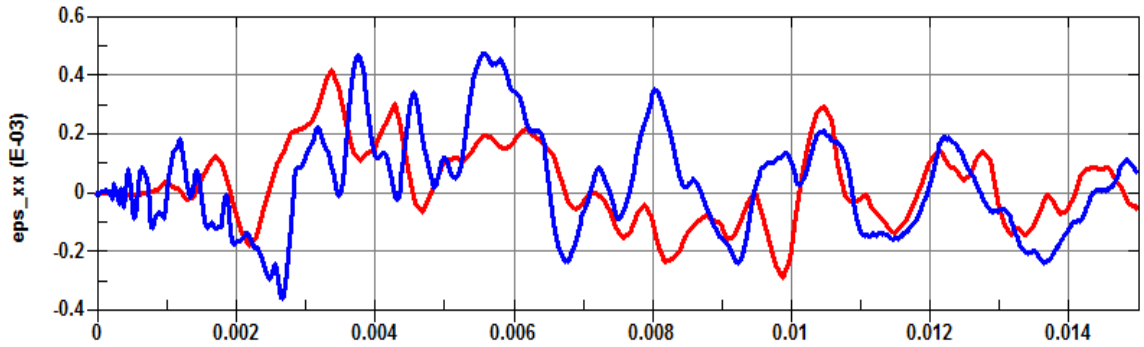

Figure 42. Comparison of strains at the side surface between the numerical and experimental results for empty box

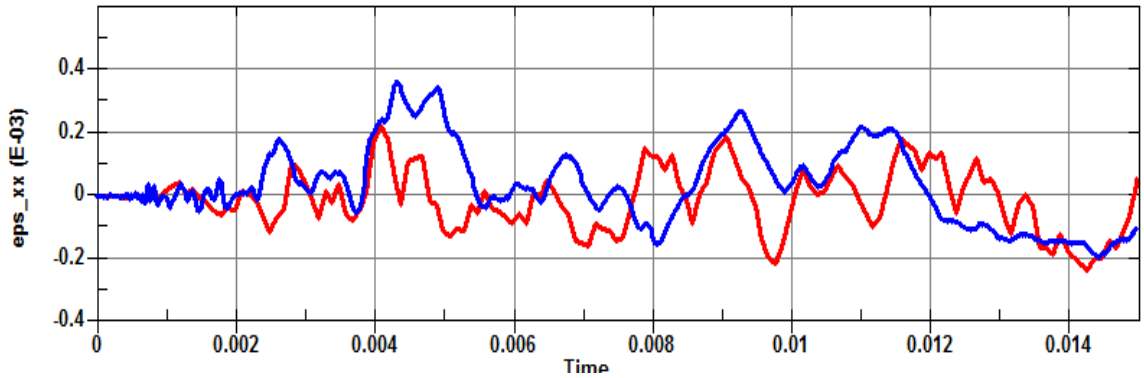

Figure 43. Comparison of strains at the back surface between the numerical and experimental results for empty box

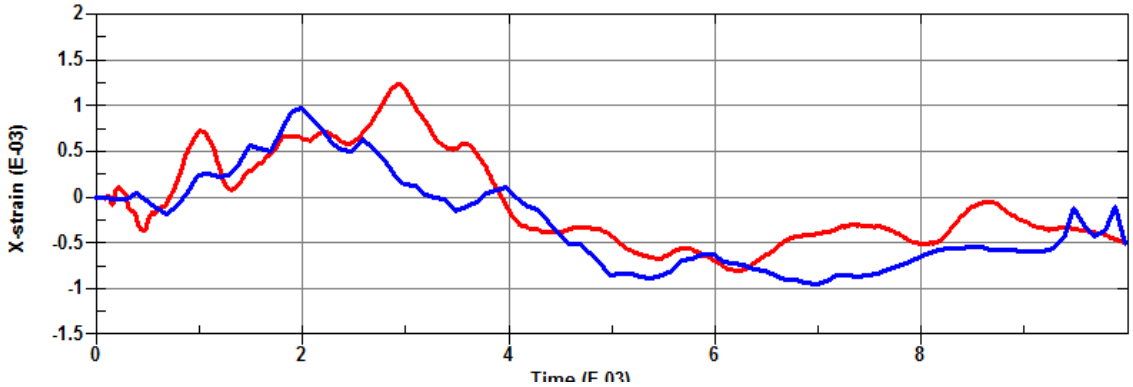

Figure 44. Comparison of strains at the front surface between the numerical and experimental results for box with 100% full water

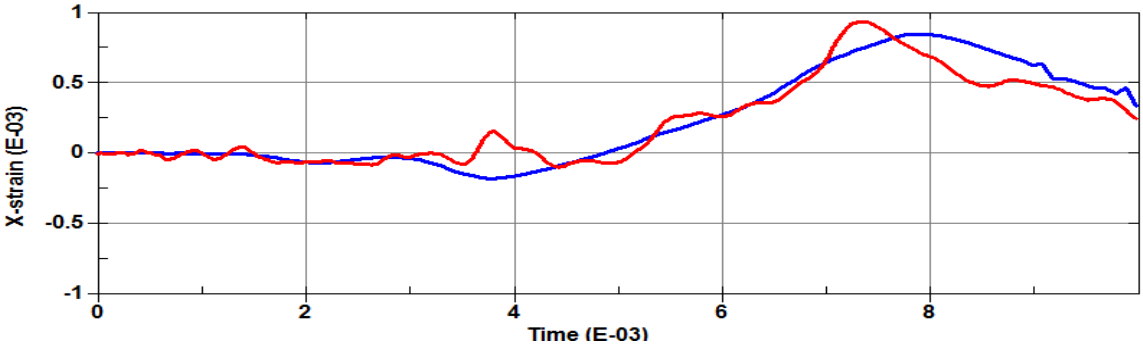

Figure 45. Comparison of strains at the side surface between the numerical and experimental results for box with 100% full water

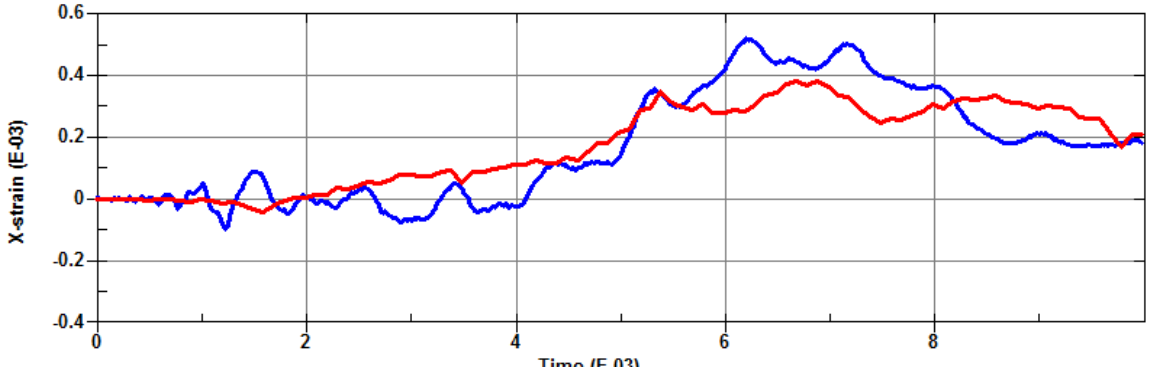

Figure 46. Comparison of strains at the back surface between the numerical and experimental results for box with 100% full water

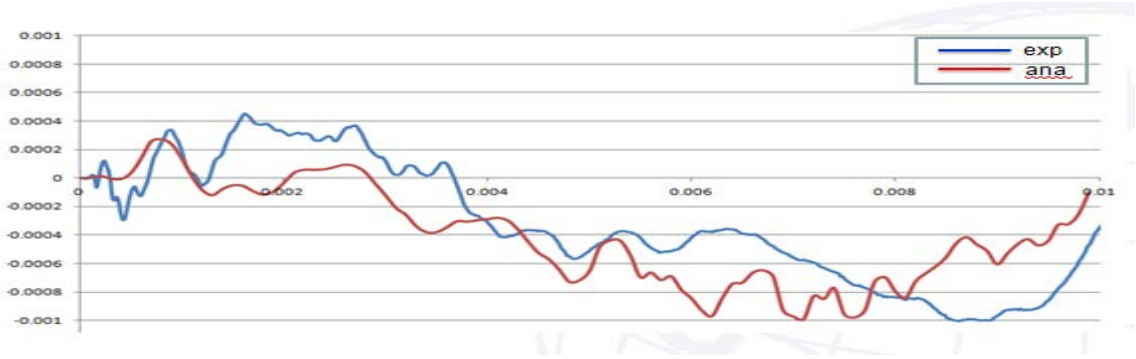

Figure 47. Comparison of strains at the front surface between the numerical and experimental results for box with 100% full water

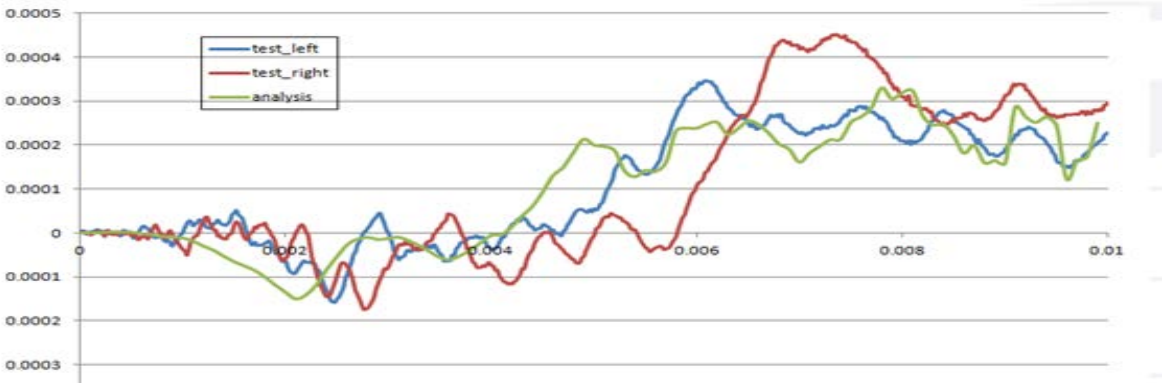

Figure 48. Comparison of strains at the side surface between the numerical and experimental results for box with 100% full water

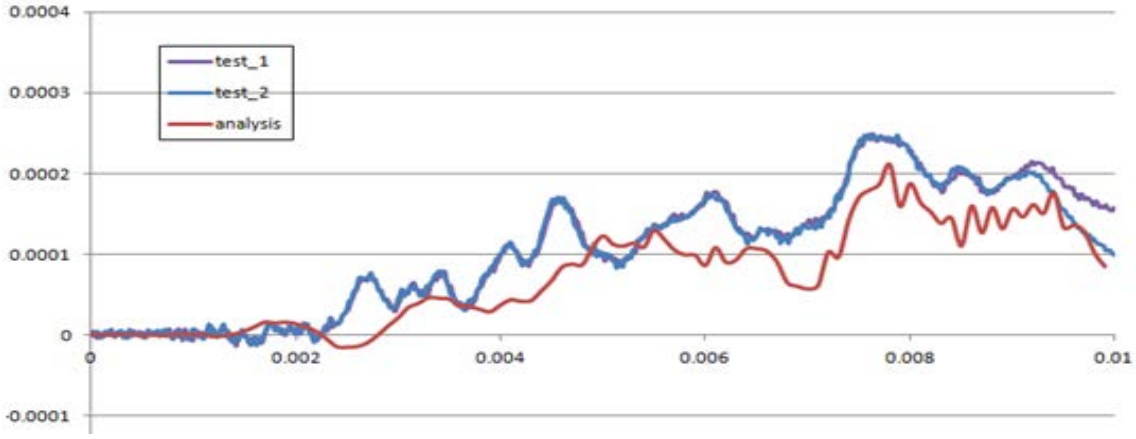

Figure 49. Comparison of strains at the back surface between the numerical and experimental results for box with 100% full water

The numerical results agreed well with the experimental data. Then, the transverse displacement at the center of the back surface was compared between the empty and 100% water-full boxes as seen in Figure 50. The internal water reduced the oscillatory motion of the back side significantly. The comparison showed that the 100% full water yielded much greater displacement with one order magnitude.

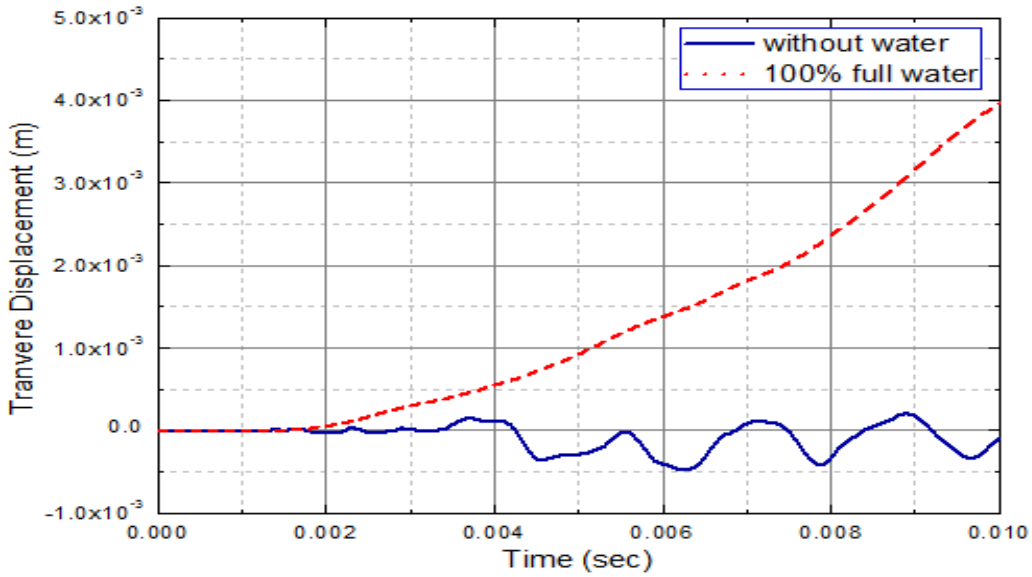

Figure 50. Comparison of transverse displacement at the back surface of the box without water and with 100% full water

Figures 51 through 53 compare deformation contours at the front, side, and back surfaces with 100% full water and without water. The deformations of the front surface were similar between the two cases at least qualitatively as shown in Figure 51 even though they were different quantitatively in terms of magnitude and frequency. Both cases vibrated in the first mode shape because the impactor hit the center of the plate. However, the side and back surfaces showed very different contour patterns. The more uniform deformation was caused by the water. Finally, the back surface has drastically different contours with and without water. The back surface without water vibrated more or less randomly while the water resulted in more regular shape of vibrations as sketched in Figure 52. The side surface without water showed asymmetric contours with larger deformation toward the impact side while the side surface with water exhibited more or less symmetric contours as shown in Figure 53.

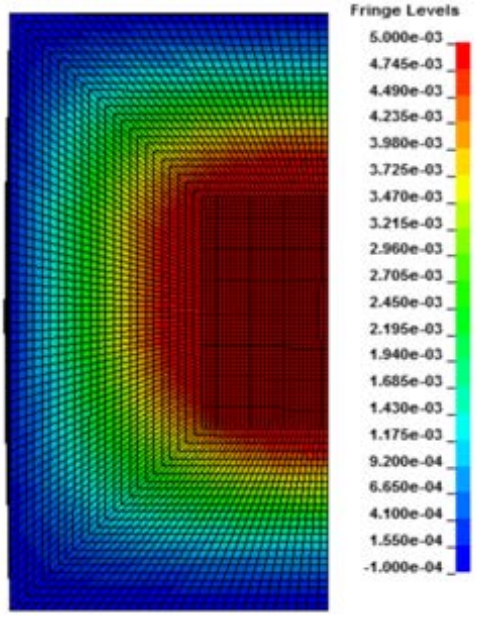

(a)

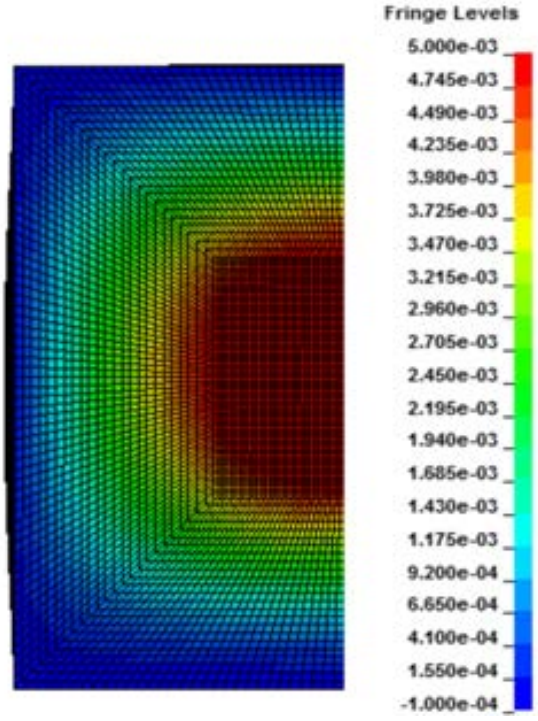

(b)

Figure 51. Comparison of contour plots of the front surface deformation (a) without water and (b) with 100% water

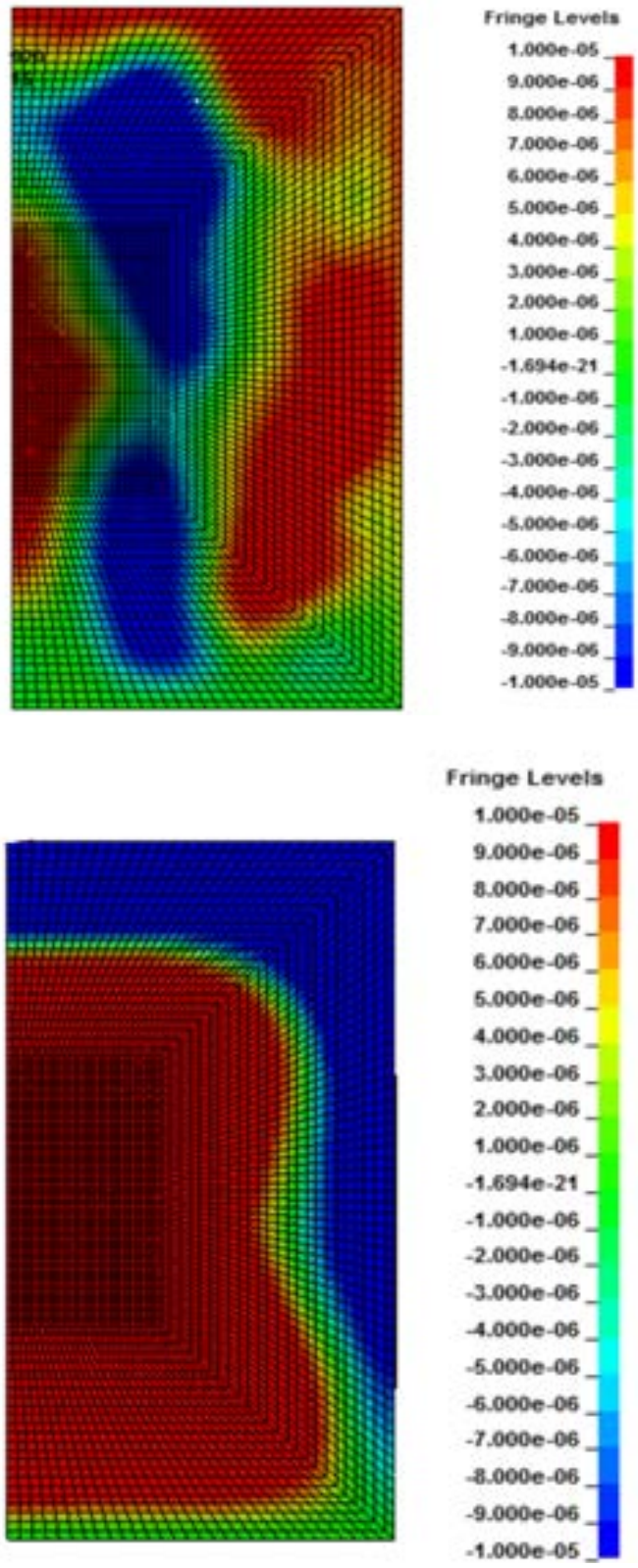

Figure 52. Comparison of plots of the back surface deformation (a) without water and (b) with 100% water

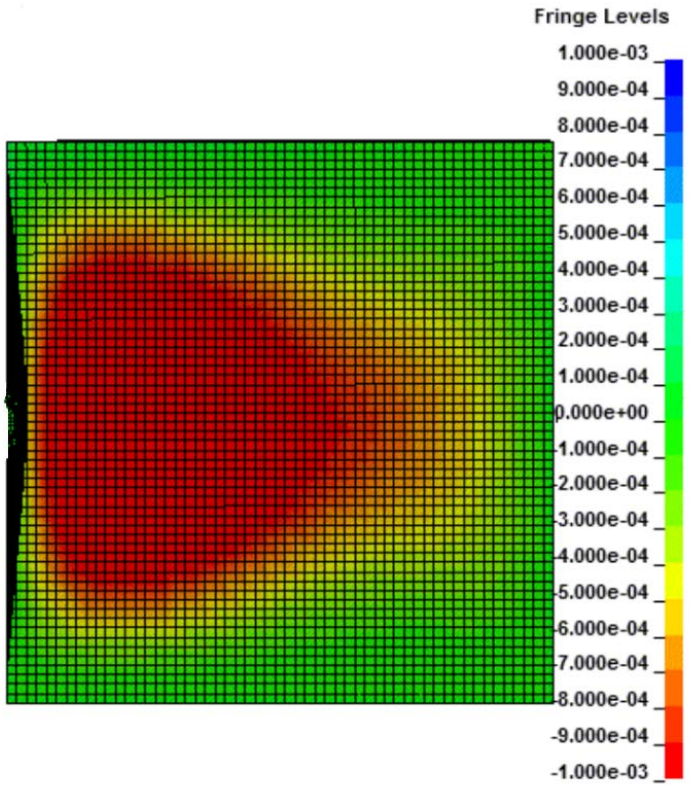

(a)

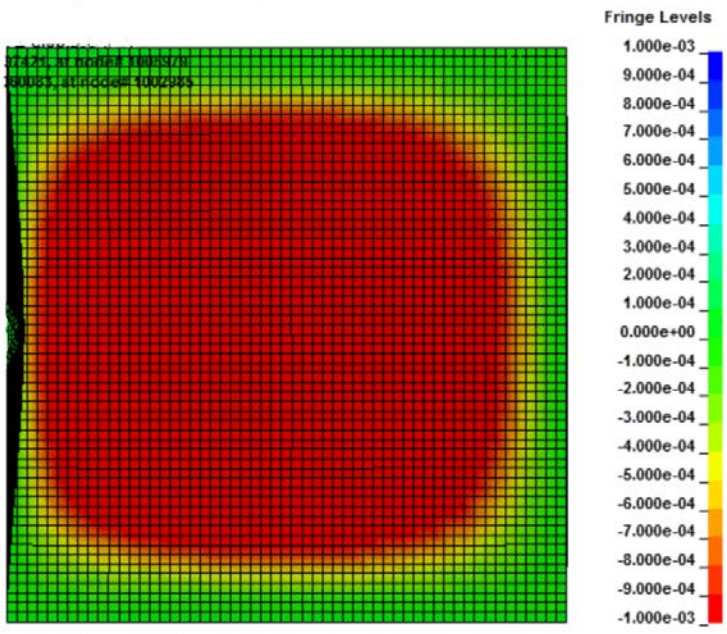

(b)

Figure 53. Comparison of contour plots of the side surface deformation (a) without water and (b) with 100% water

Another numerical study was conducted assuming the top and bottom sides constrained simultaneously. Therefore, a quarter symmetric model could be used for this study. The same impact loading was applied as before. Figure 54 compares the strains at the front surface of the empty box with two different boundary conditions; one with the bottom side constrained and the other with both top and bottom sides constrained. Constraining both top and bottom sides resulted in larger values as well as greater oscillatory variations of the strains. In other words, the movable top reduced the strain and its oscillatory motion.

On the other hand, the water inside the box with both sides constrained reached the strain-free state much faster with a very high frequency motion when compared to the other constrained case as seen in Figure 55. The most significant effect resulting from the extra top constraint occurred at the back side with the water. The strain at the back side was significantly minimized with the extra constraint as shown in Figure 56. Constraining both top and bottom sides would minimize potential failure of the back side of the box.

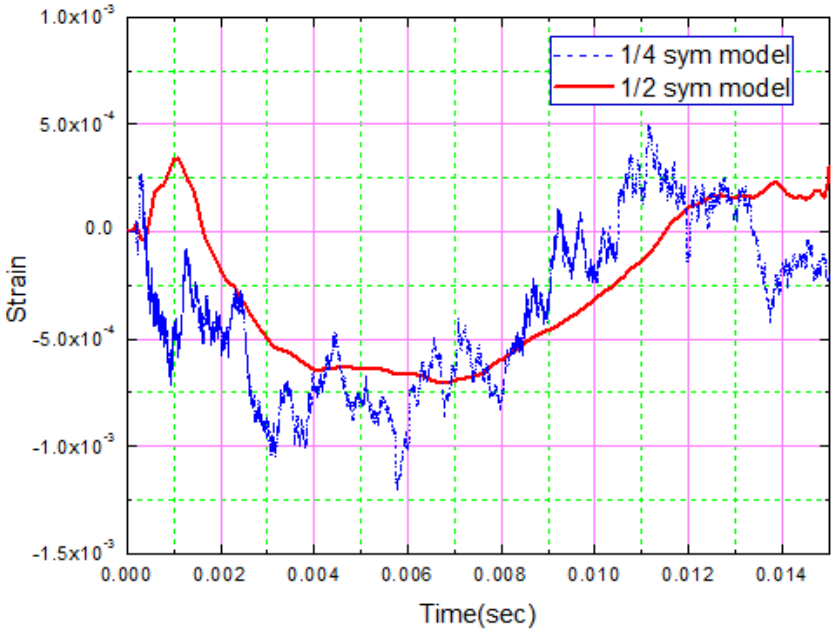

Figure 54. Comparison of strains at the front surface of the empty box with two different boundary conditions

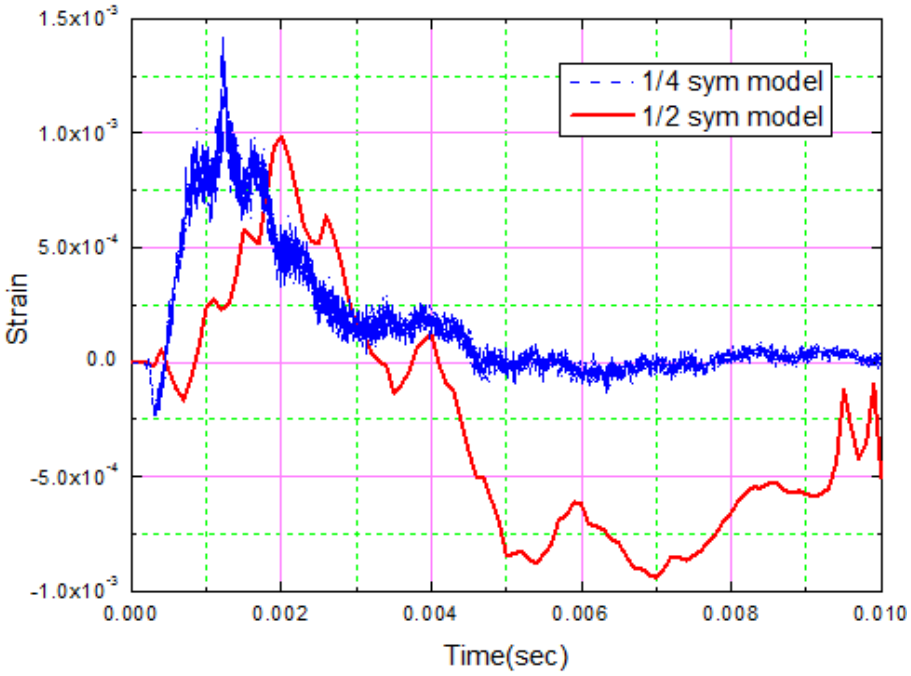

Figure 55. Comparison of strains at the front surface of the empty box with two different boundary conditions

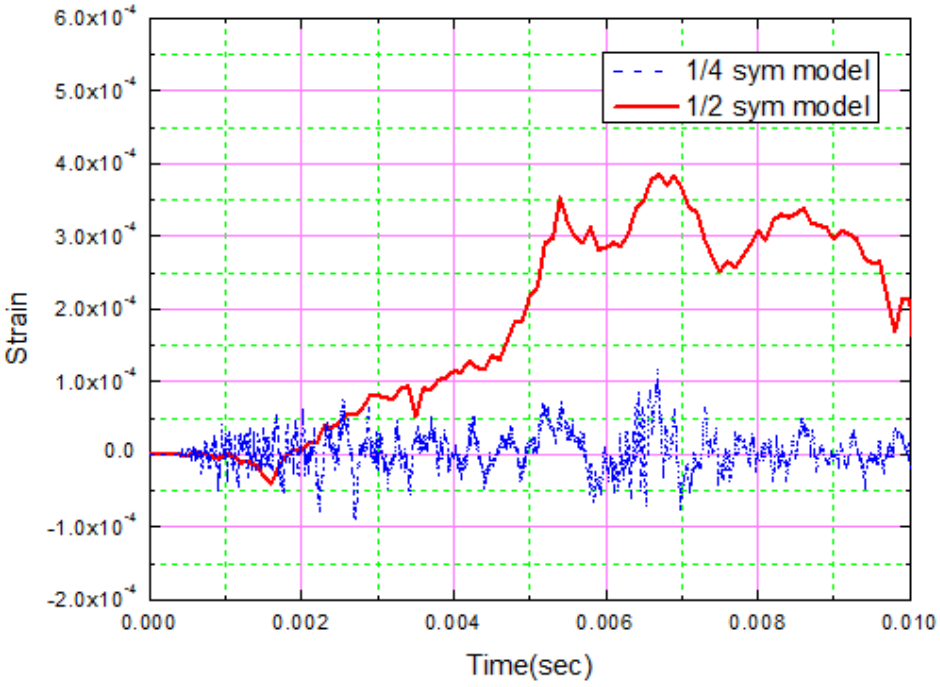

Figure 56. Comparison of strains at the back surface of the 100% water-full box with two different boundary conditions

The shock wave propagation is very important phenomenon in impact dynamics. As an example, Figure 57 shows the shock wave propagation characteristics according to the time history for 100% water filled box.

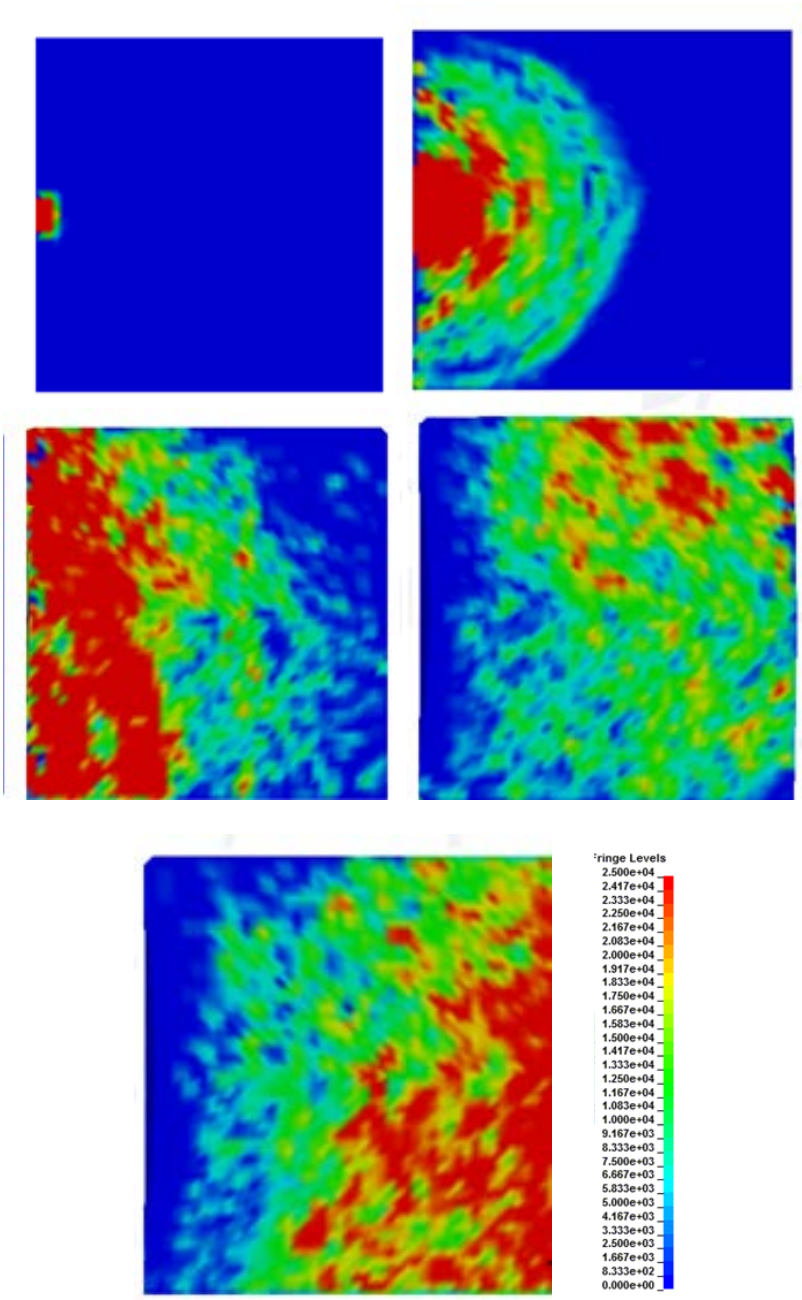

Figure 57. The shock wave propagation contour according to the time of the 100% filled water box

IV. CONCLUSIONS

A. CONCLUSIONS

The effect of fluid-structure interaction was studied experimentally and numerically for a composite box containing water, which was subjected to low velocity impacts. The water level inside the composite box was varied incrementally. The FSI played a very important role in the dynamic response of the composite box. Some important findings are summarized below. FSI had a large effect on the structural response of the composite and should be given adequate consideration in the design process for composite structures containing fluid. For the same impact mass and the initial impact velocity, the impact force was greater with more water in the box. The increase in the impact force was not linear but in the S-shape as a function of the water level inside the box. The impact side of the box reversed its motion quickly after impact and made another or multiple contacts with the impactor when the water level was at least 50%.

Comparing the deformation of each surface of the composite box with and without water showed that the back surface had the major difference due to FSI. The back surface had significant oscillation around the zero value without water while it showed much smooth and larger displacement with water. Additionally, the side surface without water vibrated with asymmetric displacement contours concentrated toward to the impact side, but with more symmetric contours with water.

The natural frequency of the box decreased as the water level increased with greater FSI effect. However, the natural frequency was also influenced with the impact loading when the water level was less than 75%. This was due to sloshing which depended on the impact level. Then, the FSI effect became different with different impact levels.

An experiment was designed and conducted to study the effects of fluid-structure interaction on a fluid-filled composite structure subjected to a low velocity impact. The fluid level was varied incrementally and two different impact velocities were tested. FSI had a significant impact on the behavior of the structural response of the composite.

Comparing the deformation of each surface of the composite box with and without water showed that the back surface had the major difference due to FSI. The back surface had significant oscillation around the zero value without water while it showed much smooth and larger displacement with water. Additionally, the side surface without water vibrated with asymmetric displacement contours concentrated toward to the impact side, but with more symmetric contours with water.

In conclusion, FSI resulted in larger deformations, strains and stresses in the composite box. As a result, composite structures containing fluids should be designed and analyzed with consideration of the effect of FSI.

B. RECOMMENDATIONS

For continued analysis and study of this topic, additional experiments and numerical simulation could be conducted to provide more information about the full field response of the structure. With additional strain gages or digital image correlation equipment the full field stress, strain, and deformation could be more accurately characterized. Additionally, the impact location and angle could be varied to determine if the effects on the structure are worsened. These results could then be compared with on-going numerical modeling and simulation to verify the structural response and dynamic behaviors.

THIS PAGE INTENTIONALLY LEFT BLANK

LIST OF REFERENCES

[1] Z. Aslan, R. Karakuzu, and B. Okutan, "The response of laminated composite plates under low-velocity impact loading," *Composite Structures*, vol. 53, pp 119-127, 2003.

[2] Y.W. Kwon, "Study of fluid effects on dynamics of composite structures," *ASME Journal of Pressure Vessel Technology*, vol. 133, pp 031301-6, 2011.

[3] MH-60L Blackhawk Walkaround. (n.d.). ARC Air. [Online]. Available: http://www.aircraftresourcecenter.com/awa01/301-400/awa338-MH-60L/00.shtm.

[4] Sang-Woo Kim, Eun-Ho Kim, Min-Soo Jeong, and In Lee, "Damage evaluation and strain monitoring for composite cylinders using tin-coated FBG sensors under low-velocity impacts," *Composites Part B*, vol. 74, pp. 13-22, 2015.

[5] M. Violette, "Fluid Structure Interaction Effect on Sandwich Composites," M.S. thesis, Naval Postgraduate School, 2011.

[6] R. Conner, "Fluid Structure Interaction Effects on Composites Under Low Velocity Impact," M.S. thesis, Naval Postgraduate School, 2012.

[7] R. McCrillis, "Dynamic Failure of Sandwich Beams with Fluid-Structure Interaction Under Impact Loading," M.S. thesis, Naval Postgraduate School, 2010.

[8] R.D. Firouz-Abadi, H. Haddadpour, and M.A. Kouchakzadeh, "Free vibrations of composite tanks partially filled with fluid," Thin-Walled Structures, vol.47, pp 1567-1574, 2009.

[9] S. Rebouillat and D. Liksonov, "Fluid-structure interaction in partially filled liquid containers: A comparative review of numerical approaches," *Computers and Fluids*, vol. 39, pp 739-746, 2010.

[10] Hyun Moo Koh, Jae Kwan Kim, and Jang-Ho Park, "Fluid-structure interaction analysis of 3-D rectangular tanks by a variationally coupled BEM-FEM and comparison with test results," Earthquake Engineering and Structural Dynamics, vol. 27, pp. 109-124, 1998.

[11] M. Eswaran, U.K. Saha, and D. Mairy, "Effect of baffles on a partially filled cubic tank: Numerical simulation and experimental validation," *Computers and Structures*, vol. 87, pp. 198-205, 2009.

[12] F. Ince, H.S. Turkmen, Z. Mecitoglu, N. Uludag, I. Durgun, E. Altinok, and H. Orenel, "A numerical and experimental study on the impact behavior of box structures," Engineering Procedia, vol. 10, pp 1736-1741, 2011.

[13] J.A. Artero-Guerrero, J. Pernas-Sanchez, J. Lopez-Puente, and D. Varas, "On the influence of filling level in CFRP aircraft fuel tank subjected to high velocity impacts," *Composite Structures*, vol. 107, pp. 570-577, 2014.

[14] J.A. Artero-Guerrero, J. Pernas-Sanchez, J. Lopez-Puente, D. Varas, "Numerical analysis of CFRP fluid-filled tubes subjected to high-velocity impact," *Composite Structures*, vol. 96, pp. 286-297, 2013.

[15] D. Varas, R. Zaera, and J. Lopez-Puente, "Experimental study of CFRP fluid-filled tubes subjected to high-velocity impact," *Composite Structures*, vol. 93, pp. 2598-2609, 2011.

[16] Y. W. Kwon, "Study of fluid effects on dynamics of composite structures", ASME Journal of Pressure Vessel Technology, Vol. 133, June 2011, pp. 031301-6.

[17] N. Pal, S. Bhattacharyya, and P. Sinha, "Coupled slosh dynamics of liquid-filled, composite cylindrical tanks", Journal of Engineering Mechanics**,** April 1999, Vol. 125, No. 4 : pp. 491-495

[18] S.W. Gong, and K.Y. Lam, "Transient response of floating composite ship section subjected to underwater shock", Composite Structures, Vol. 46, Issue 1, September 1999, pp. 65-71.

[19] Y. W. Kwon, M. A. Violette, R. D. McCrillis, and J. M. Didoszak, "Transient Dynamic Response and Failure of Sandwich Composite Structures under Impact Loading with Fluid Structure Interaction", Applied Composite Materials. Vol. 19, No. 6, 2012, pp. 921-940.

[20] L. E. Craugh and Y. W. Kwon, "Coupled Finite Element and Cellular Automata Methods for Analysis of Composite Structures with Fluid-Structure Interaction", Composite Structures, Vol. 102, August 2013, pp. 124-137.

[21] Y. W. Kwon, E. M. Priest, J. H. Gordis, "Investigation of vibrational characteristics of composite beams with fluid-structure interaction", Composite Structures, Vol. 105, 2013, pp. 269-278.

[22] R.D. Firouz-Abadi, H. Haddadpour, and M.A. Kouchakzadeh, "Free vibrations of composite tanks partially filled with fluid," Thin-Walled Structures, vol.47, pp 1567-1574, 2009.

[23] G.A. Schoeppner and S. Abrate, "Delamination threshold loads for low velocity impact on composite laminates", Composites Part A: Applied Science and Manufacturing, Volume 31, Issue 9, September 2000, pp. 903–915

[24] H.-Y. T. Wu and G. S. Springer, “Measurements of matrix cracking and delamination caused by impact on composite plates”, Journal of Composite Materials, Vol. 22, No. 6, June 1988, pp. 518-532.

[25] L. Lammerant, and I. Verpoest, “Modelling of the interaction between matrix cracks and delaminations during impact of composite plates”, Composites Science and Technology, Vol. 56, Issue 10, 1996, pp. 1171–1178.

[26] Sang-Woo Kim, Eun-Ho Kim, Min-Soo Jeong, and In Lee, “Damage evaluation and strain monitoring for composite cylinders using tin-coated FBG sensors under low-velocity impacts,” Composites Part B, vol. 74, pp. 13-22, 2015.

[27] D. Varas, R. Zaera, and J. Lopez-Puente, “Experimental study of CFRP fluid-filled tubes subjected to high-velocity impact,” Composite Structures, vol. 93, pp. 2598-2609, 2011.

[28] J.A. Artero-Guerrero, J. Pernas-Sanchez, J. Lopez-Puente, D. Varas, “Numerical analysis of CFRP fluid-filled tubes subjected to high-velocity impact,” Composite Structures, vol. 96, pp. 286-297, 2013.

[29] J.A. Artero-Guerrero, J. Pernas-Sanchez, J. Lopez-Puente, and D. Varas, “On the influence of filling level in CFRP aircraft fuel tank subjected to high velocity impacts,” Composite Structures, vol. 107, pp. 570-577, 2014.

[30] LS-DYNA Keyword User’s Manual, Livermore Software Technology Corporation,March 2015.

THIS PAGE INTENTIONALLY LEFT BLANK

INITIAL DISTRIBUTION LIST

1. Defense Technical Information Center
   Ft. Belvoir, Virginia

2. Dudley Knox Library
   Naval Postgraduate School
   Monterey, California

3. Research Sponsored Programs Office, Code 41
   Naval Postgraduate School
   Monterey, CA 93943

4. Young W. Kwon
   Naval Postgraduate School
   Monterey, CA 93943

5. Taylor J. South
   Naval Postgraduate School
   Monterey, CA 93943

6. Kyoung Jae Yun
   Agency for Defense Development
   Yuseong, Korea